AD-A236 999

(2)

REPORT DOCUMENTATION PAGE

READ INSTRUCTIONS BEFORE COMPLETING FORM

1. REPORT NUMBER # 22	RECIPIENT'S CATALOG NUMBER
4. TITLE (and Subtitle) An Extension of a Kinetic Theory of Polymer Crystallization Through the Exclusion of Negative Barriers	5. TYPE OF REPORT & PERIOD COVERED Technical
	6. PERFORMING ORG. REPORT NUMBER
7. AUTHOR(s) Louis Petrone, Jerry I. Scheinbeim and Brian A. Newman	8. CONTRACT OR GRANT NUMBER(s) N00014-88-K-0122
9. PERFORMING ORGANIZATION NAME AND ADDRESS Dept. of Mechanics and Materials Science College of Engineering, Rutgers University Piscataway, New Jersey 08855-0909	10. PROGRAM ELEMENT, PROJECT, TASK AREA & WORK UNIT NUMBERS
11. CONTROLLING OFFICE NAME AND ADDRESS Dr. Joanne Milliken Office of Naval Research Arlington, VA 22217-5000	12. REPORT DATE
	13. NUMBER OF PAGES 35
14. MONITORING AGENCY NAME & ADDRESS(if different from Controlling Office)	15. SECURITY CLASS. (of this report) UNCLASSIFIED
	15a. DECLASSIFICATION/DOWNGRADING SCHEDULE

16. DISTRIBUTION STATEMENT (of this Report)

Approved for public release; distribution unlimited. Reproduction in whole or in part is permitted for any purpose of the United States Government.

17. DISTRIBUTION STATEMENT (of the abstract entered in Block 20, if different from Report)

18. SUPPLEMENTARY NOTES

Submitted, Macromolecules

91-01970

19. KEY WORDS (Continue on reverse side if necessary and identify by block number)

20. ABSTRACT (Continue on reverse side if necessary and identify by block number)

The simplest version of the Lauritzen-Hoffman (LH) model of polymer crystallization which applies to infinitely long model polymer molecules crystallizing on an existing substrate of infinite width, is re-examined. The mathematical expressions for the model free energy barriers are observed to take on negative values at high supercooling. Since such negative barriers appear to be physically unrealizable for the crystallization process, the LH model is extended by imposing a mathematical constraint on the expressions for the barriers, to

OVER

DD FORM 1 JAN 73 1473 91 6 12 049

UNCLASSIFIED

SECURITY CLASSIFICATION OF THIS PAGE (When Data Entered) forbid them from ever being negative. The extended model contains one parameter γ which varies from zero to one and is analogous to the parameter ψ of the LH model. For all values of γ less than one, the extended model predicts a finite lamellar thickness at every supercooling; moreover, this thickness, at large undercooling, decreases monotonically with increasing undercooling in agreement with experiment, but in marked contrast to the LH model which exhibits the well-known $\delta\ell$ catastrophe. The relative insensitivity of the calculated lamellar thicknesses to the parameter γ supports the use of $\gamma = 0$ as a first approximation for mathematical convenience in practice.

OFFICE OF NAVAL RESEARCH

Contract N00014-88-K-0122

Technical Report No. 22

An Extension of a Kinetic Theory of Polymer Crystallization Through the Exclusion of Negative Barriers

by

Louis Petrone, Jerry I. Scheinbeim and Brian E. Newman

Prepared for Publication in

Macromolecules

Department of Mechanics and Materials Science
College of Engineering
Rutgers University
Piscataway, NJ 08855-0909

May 1991

ABSTRACT

The simplest version of the Lauritzen-Hoffman (LH) model of polymer crystallization which applies to infinitely long model polymer molecules crystallizing on an existing substrate of infinite width is reexamined. The mathematical expressions for the model free energy barriers are observed to take on negative values at high supercooling. Since such negative barriers appear to be physically unrealizable for the crystallization process, the LH model is extended only by imposing a mathematical constraint on the expressions for the barriers to forbid them from ever being negative. The extended model contains one parameter γ which varies from zero to one and is analogous to the parameter ψ of the LH model. For all values of γ less than one, the extended model predicts a finite lamellar thickness at every supercooling; moreover, this thickness, at large undercooling decreases monotonically with increasing undercooling in agreement with experiment but in marked contrast to the LH model which exhibits the well-known $\delta \ell$ catastrophe. The relative insensitivity of the calculated lamellar thicknesses to the parameter γ supports the use of low parameter values such as zero as a first approximation for mathematical convenience in practice.

I. INTRODUCTION

Recently, the isothermal (unoriented) crystallization of poly(vinylidene) fluoride (PVF_2) from the melt in the presence of a high static electric field has been studied experimentally and theoretically as a simple model system for the investigation of the structure-property relationships of this polymer.[I.1,I.2] Of the four well-known crystalline forms α, β, γ, and δ (or II, I, III, and IV) of PVF_2; however, the phase which has the greatest potential for applications <u>via</u> its large spontaneous polarization[I.2] is not produced on crystallization from the melt. This phase--namely β--has been observed to exhibit highly oriented growth (mixed with some unoriented α phase growth) during the initial stages of crystallization from solution under a high static field of highly plasticized PVF_2 (i.e. of a concentrated solution of tricresyl phosphate and PVF_2 in which the tricresyl phosphate content decreases by evaporation); at longer times, the formation of the nonpolar α phase predominates.[I.3] The decrease in plasticizer content and the subsequent crystal growth behavior implies that the local electric field in the solution region changes. As part of the continuing effort simply to understand the structure-property relationships of PVF_2 and because of its practical importance, our ultimate goal--despite the complexity of the system described--is to develop a theory or model which can account for its crystallization behavior.

As in the case of isothermal crystallization of α and γ phase from the melt in an electric field,[I.2] a theory of isothermal crystallization of α, β, and δ phase from concentrated solution in an electric field would be based on "classical" and "polymer" theories of nucleation and growth in the absence of an applied field. Most importantly, the nucleation barrier or activation free energy barrier for nucleation would certainly be different in the presence of the field than in its absence; and this barrier has been seen to be of fundamental importance in the theories of polymer crystallization, the simplest of which is the LH or Lauritzen-Hoffman theory.[1-3] One possibly unrealistic feature which seems to have been incorporated into this theory in order to simplify it is that the nucleation barrier is not constrained in the theory to take on only nonnegative values. The word "barrier" connotes a positive quantity, and furthermore, the LH theory is based on transition state theory in which the barrier corresponds to an intermediate configuration or transition state of the system which is at a free energy maximum relative to some initial and final state of the system.[4] Moreover, the LH theory exhibits, in contrast with experiment, the $\delta\ell$ catastrophe wherein the calculated average lamellar thickness $\bar{\ell}$ suddenly passes through a minimum and becomes infinite at a temperature, T_c, corresponding to a moderately large undercooling; and, in fact, the nucleation barrier in this theory is positive for all $T > T_c$, is zero at $T = T_c$, and is negative for all $T < T_c$ for the special case which Lauritzen and Hoffman [4,5] have recently considered. Therefore, prior to developing an extension of the LH theory which would involve ascertaining the effect of an electric field on the nucleation barrier, we try to extend the LH theory to larger undercooling by incorporating into it the assumption that free energy barriers cannot be negative. Note that, unlike in the LH theory of polymer crystallization, barriers in classical nucleation theory are never negative; however, the classical theory does not explicitly take into account polymer chain folding, and for that reason, we have not yet considered modifying the Marand and Stein theory[I.1] of crystallization from the melt to treat the PVF_2/tricresyl phosphate crystallizing solution.

The remainder of this paper is organized as follows. In Section II, the LH model is described. The kinetic treatment of the LH model is given in Section III. The rate constants needed for this treatment are determined in Section IV. Next, our extension of the LH model is described in Section V; the conditions which determine the sign of $\Delta\phi_1$, the free energy of formation of that portion of a model polymer molecule which crystallizes first on an existing crystal, are found in Section VI. A summary of the expressions for the barriers in our model is given in Section VII along with the expressions for the average lamellar thickness. In Section VIII, the variable transformations required as a preliminary to numerical integration are introduced. Results and discussion appear in Section IX, and conclusions are given in Section X.

II. THE LAURITZEN-HOFFMAN MODEL

The model to be extended is one version[1,2] of the well-known Lauritzen-Hoffman (LH) model of polymer crystallization. Our description of this version is as follows. The model polymer molecules are assumed to be infinitely long and crystallize on an existing crystalline face or substrate which is assumed to be infinitely wide (i.e. the fact that its width is finite is ignored). A sequence of length ℓ of polymer segments of width a and thickness b as well as the volume associated with that sequence--which is taken to be a parallelepiped of length ℓ, width a, and thickness b--is designated as a stem. Only stems of length ℓ can crystallize on an existing face of length ℓ, but the length ℓ, the lamellar thickness, can vary from crystal to crystal. (Of course, a and b cannot vary from face to face.) <u>Any</u> sequence of length ℓ of segments of a model molecule can be placed first on a given face and upon placement, is designated as the first stem. The free energy of formation of the first stem is

$$\Delta\phi_1 - \Delta\phi_0 = \Delta\phi_1 - 0 \quad \text{or} \quad \Delta\phi_1 = 2ab\sigma'_e + 2b\ell\sigma - ab\ell\Delta f$$

where $\Delta f > 0$ is the free energy of fusion per unit volume at a temperature T below the melting point T_m° of a crystal of very large ℓ ($\Delta f = 0$ at $T = T_m^\circ$), where σ is the lateral surface free energy per unit area (i.e. that associated with the surfaces of area $b\ell$ and $a\ell$ of a stem), and where σ'_e is the surface free energy per unit area associated with the cilium that protrudes through each of the surfaces of area ab of the first stem. Recently,[1-3] σ'_e has been assumed to be zero; generally, one can have[6] $0 \le \sigma'_e \le \sigma_e$. All surface free energies per unit area in the model are assumed to be independent of T and ℓ.

(See Figure 2(a) of Reference 1 or Figure 22 of Reference 2.) The placement of each subsequent stem involves:

1. the destruction of the cilium associated with one of the surfaces of area ab of an adjacent stem already crystallized,
2. an adjacent reentry and the formation of a tight fold associated with two surfaces of area ab, and
3. the formation of a cilium associated with the remaining surface of area ab of the stem being placed.

Only adjacent reentry and hence only tight folding is incorporated in this version of the model.

The free energy of formation of the νth stem ($\nu > 1$) is therefore

$$\Delta\phi_\nu - \Delta\phi_{\nu-1} = -ab\sigma_e' + 2ab\sigma_e + ab\sigma_e' - ab\ell\Delta f$$

or

$$\Delta\phi_\nu - \Delta\phi_{\nu-1} = 2ab\sigma_e - ab\ell\Delta f = -E$$

where $\Delta\phi_\nu$ is the free energy of formation of a group of ν stems (relative to $\Delta\phi_0 = 0$) and where σ_e is the surface free energy per unit area associated with half of a fold. Iteration of $\Delta\phi_\nu = \Delta\phi_{\nu-1} - E \quad (\nu > 1)$ gives

$$\Delta\phi_\nu = \Delta\phi_1 - (\nu-1)E$$

$$= 2b\ell\sigma + 2ab\sigma_e' - 2ab\sigma_e + \nu ab(2\sigma_e - \ell\Delta f).$$

In order that stem additions subsequent to the placement of the first stem be thermodynamically favorable, i.e. in order that they would in fact occur, one must impose the constraint $E > 0$ and consequently $\ell > \frac{2\sigma_e}{\Delta f}$. By contrast, $\Delta\phi_1$ can be positive, zero, or negative; $E > 0$ guarantees that $\Delta\phi_\nu < 0$ will occur for finite ν. Note the sign conventions for $\Delta\phi_1$ and E.

III. THE KINETIC TREATMENT OF THE LAURITZEN-HOFFMAN MODEL

Our description of the kinetic treatment[1,2] of the LH model is as follows. The following assumptions are made:

1. Assume that transition state theory can be utilized to describe the kinetics of the LH model of polymer crystallization.
2. Assume that the formation (crystallization) of a single stem is an elementary process or elementary reaction; that the destruction (melting) of a single stem is an elementary process or elementary reaction; and that transition state theory can be applied to these two elementary processes with a single transition state corresponding to a relative free energy maximum or barrier thus occurring between each two integral values of ν on a plot of $\Delta\phi_\nu$ vs. ν.
3. Assume that only one stem at a time can be formed or destroyed.

The kinetic problem is to derive an expression for the net rate $S_\nu(\ell,T)$ at which stems of length ℓ (and width a) pass over or surmount the νth free energy barrier at temperature T. The problem requires consideration of the following set of connected elementary reactions

$$0 \underset{B_1}{\overset{A_0}{\rightleftarrows}} 1 \underset{B}{\overset{A}{\rightleftarrows}} 2 \underset{B}{\overset{A}{\rightleftarrows}} 3 \underset{B}{\overset{A}{\rightleftarrows}} 4 \ldots$$

where A is the rate constant for the forward reaction $\nu \rightarrow \nu+1$ ($\nu \geq 1$) and B is that for the reverse reaction $\nu+1 \rightarrow \nu (\nu \geq 1)$, and where A_0 and B_1 are the analogous rate constants for the $\nu=0 \rightleftarrows \nu=1$ reactions. Solution[1] of this problem in the steady-state approximation gives

$$S_\nu(\ell,T) = \frac{N_0 A_0 (A-B)}{A-B+B_1} = S(\ell,T)$$

for all ν, where N_0 is the number of sites or locations available for the placement of a first stem. The total net rate at which stems (i.e. the net rate including stems of all possible values of ℓ) pass over the νth barrier at temperature T is given, for all ν, by

$$S_{Total}(T) = \sum_{\ell=\ell_1}^{\infty} S(\ell,T)$$

where ℓ_1 is the smallest allowed value of ℓ which satisfies the constraint $\ell > \frac{2\sigma_e}{\Delta f}$. Note that ℓ is a discrete variable--the smallest increment in ℓ that can be made is the monomer repeat length ℓ_u. To find ℓ_1, first write $\ell = m\ell_u$, where m is a positive integer and then realize that, since ℓ must exceed $\frac{2\sigma_e}{\Delta f}$, the smallest value of m must be equal to the smallest integer greater than $\left(\frac{2\sigma_e/\Delta f}{\ell_u}\right)$. Therefore, $\ell_1 = \left[1+E(x)\right]\ell_u$, where $x = \frac{2\sigma_e/\Delta f}{\ell_u}$ and E(x) designates the integer part of x. Substituting $\ell_u = \frac{2\sigma_e}{x\Delta f}$ into the expression for ℓ_1 gives $\ell_1 = \left[\frac{1+E(x)}{x}\right]\left(\frac{2\sigma_e}{\Delta f}\right)$. To a good approximation, $\frac{1+E(x)}{x} \approx 1$ (i.e. x is sufficiently greater than 1) so that $\ell_1 \approx \frac{2\sigma_e}{\Delta f}$.

Finally, one assumes that $\sum_{\ell=\ell_1}^{\infty} S(\ell,T) \approx \frac{1}{\ell_u}\int_{\ell_1}^{\infty} S(\ell,T)d\ell$; and the kinetically-determined *average* lamellar thickness is then given by

$$\bar{\ell}(T) = \frac{\int_{\ell_1}^{\infty} \ell\ S(\ell,T)\ d\ell}{\int_{\ell_1}^{\infty} S(\ell,T)\ d\ell}.$$

IV. DETERMINATION OF THE RATE CONSTANTS

To obtain expressions for A_0, B_1, A_1 and B, one must first determine expressions for the free energy barriers for the relevant reactions $\nu \rightleftarrows \nu+1$ ($\nu \geq 0$). Let E_1 be the free energy barrier to the destruction of the first stem; then $\Delta\phi_1 + E_1$ is the barrier to the formation of the first stem in order that $(\Delta\phi_1+E_1) - E_1 = \Delta\phi_1$. Let E_2 be the free enrgy barrier to the formation of each subsequent stem; then $E + E_2$ is the barrier to the destruction of each such stem in order that $(E+E_2) - E_2 = E$. Now one does not know the free energy barrier to the formation of the first stem. At least, one does know that it depends on what length ℓ' of a fully adsorbed stem of length ℓ

actually crystallizes before the barrier is surmounted. If $\ell' = 0$, then none of the free energy of fusion is released before the barrier is surmounted, and clearly, $\Delta\phi_1 + E_1 = 2ab\sigma_e' + 2b\ell\sigma$ and $E_1 = ab\ell\Delta f$. In general then, for $0 \le \ell' \le \ell$, $\Delta\phi_1 + E_1 = 2ab\sigma_e' + 2b\ell\sigma - ab\ell'\Delta f$ and $E_1 = ab(\ell-\ell')\Delta f$. Since ℓ' is unknown, a parameter $\psi = \frac{\ell'}{\ell}$ with $0 \le \psi \le 1$, is introduced in order that all possible so-called apportionments of the free energy of fusion $ab\ell\Delta f$ between the rate constants for the formation and destruction of a first stem (i.e. for the forward and reverse reactions $0 \rightleftarrows 1$) can be considered. Thus,

$$\Delta\phi_1 + E_1 = 2ab\sigma_e' + 2b\ell\sigma - \psi ab\ell\Delta f \quad \text{and} \quad E_1 = (1-\psi)\, ab\ell\Delta f.$$

Note that the greater the amount $\psi ab\ell\Delta f$ of the free energy of fusion which is in fact "apportioned" (i.e. the greater the value of ψ or ℓ'), the smaller the value of both $\Delta\phi_1 + E_1$ and E_1 (for a given ℓ and T). A very similar interpretation of ψ has been discussed recently.[3]

Similarly, for each subsequent stem, let ℓ'' $(0 \le \ell'' \le \ell)$ be the length of a fully adsorbed stem which actually crystallizes before the barrier to the formation of the stem is surmounted. Then $E_2 = 2ab\sigma_e - ab\ell''\Delta f$ and $E + E_2 = ab(\ell-\ell'')\Delta f$. Define the apportionment parameter $\hat{\psi} = \frac{\ell''}{\ell}$ with $0 \le \hat{\psi} \le 1$ so that

$$E_2 = 2ab\sigma_e - \hat{\psi} ab\ell\Delta f \quad \text{and} \quad E + E_2 = (1-\hat{\psi})\, ab\ell\Delta f.$$

Finally, utilizing transition state theory,

$$A_0 = \frac{kT}{h}\, e^{-(\Delta\phi_1+E_1+\Delta\hat{F})/kT} = \beta\, e^{-(\Delta\phi_1+E_1)/kT}$$

$$B_1 = \beta\, e^{-E_1/kT} \quad , \quad A = \beta\, e^{-E_2/kT} \quad , \quad B = \beta\, e^{-(E+E_2)/kT}$$

where $\Delta\hat{F}$ is the contribution to <u>each</u> barrier as a result of retardations in the transport of a polymer chain through the liquid to the substrate or vice versa. Note that $\frac{B}{A}$ does not depend on $\hat{\psi}$ and that $\frac{B_1}{A_0}$ does not depend on ψ as required.

V. THE EXTENSION OF THE LAURITZEN-HOFFMAN MODEL

As implied throughout the above discussion, the application of transition state theory to the elementary processes of single stem formation and destruction presumes that there is a single relative free energy maximum[4] or barrier between each two integral values of ν on a plot of $\Delta\phi_\nu$ vs. ν. Consequently, $\Delta\phi_1+E_1$, E_1, E_2, and $E+E_2$ should never be negative. learly, $E_1 = (1-\psi)\, ab\ell\Delta f$ and $E+E_2 = (1-\hat{\psi})ab\ell\Delta f$ are never negative; however, the expressions given above for $\Delta\phi_1+E_1$ and E_2 can be negative. In fact, E_2, for example, is negative for all ℓ such that $\frac{2\sigma_e}{\hat{\psi}\Delta f} < \ell \le \infty$ for a given Δf, $\hat{\psi}$, and σ_e. We propose to extend the LH model by incorporating into the model the assumption that free energy barriers cannot be negative, i.e. only apportionments of the free energy of fusion which result in a nonnegative barrier will be allowed.

In order to incorporate this constraint into the model, first note that $\Delta\phi_1+E_1 = 2ab\sigma_e' + 2b\ell\sigma - \psi ab\ell\Delta f$ is never negative when $\Delta\phi_1$ is positive since then, $ab\ell\Delta f < 2ab\sigma_e' + 2b\ell\sigma$ always holds and $\psi ab\ell\Delta f < 2ab\sigma_e' + 2b\ell\sigma$ follows. However, when $\Delta\phi_1$ is negative, the expression $2ab\sigma_e' + 2b\ell\sigma - \psi ab\ell\Delta f$ can be negative. The requirement that $\Delta\phi_1 + E_1 \ge 0$ hold when $\Delta\phi_1$ is negative implies that one is not allowed to apportion all of the free energy of fusion $ab\ell\Delta f$ when $\Delta\phi_1$ is negative. If the amount $\psi ab\ell\Delta f$ of the free energy of fusion which is apportioned were to exceed $2ab\sigma_e' + 2b\ell\sigma$, then $\Delta\phi_1+E_1$ would be negative. The maximum amount which can be apportioned is indeed $2ab\sigma_e' + 2b\ell\sigma$, and therefore one has, when $\Delta\phi_1 < 0$,

$$\Delta\phi_1+E_1 = \xi(2ab\sigma_e' + 2b\ell\sigma)$$

where ξ is an apportionment parameter with $0 \le \xi \le 1$. Using $(\Delta\phi_1+E_1) - E_1 = \Delta\phi_1$ or $E_1 = (\Delta\phi_1+E_1) - \Delta\phi_1$ gives

$$E_1 = \xi(2ab\sigma_e' + 2b\ell\sigma) - (2ab\sigma_e' + 2b\ell\sigma - ab\ell\Delta f) = ab\ell\Delta f - (1-\xi)(2ab\sigma_e' + 2b\ell\sigma).$$

Observe that the requirement that $\Delta\phi_1+E_1 \geq 0$ holds when $\Delta\phi_1$ is negative is equivalent to the physically realistic requirement that the barrier E_1 to the destruction of the first stem cannot be smaller than the free energy increase $(-\Delta\phi_1)$ that occurs upon its destruction. (Note that $ab\ell\Delta f-(2ab\sigma_e'+2b\ell\sigma) = -\Delta\phi_1$.) Also, this physically realistic requirement implies that an adsorbed first stem cannot completely crystallize before the barrier to the formation of that stem is surmounted, i.e. that the upper limit on ℓ' is less than ℓ when $\Delta\phi_1$ is negative. (This upper limit on ℓ' is determined later.) For $\Delta\phi_1 > 0$, the expressions $\Delta\phi_1 + E_1 = 2ab\sigma_e' + 2b\ell\sigma - \psi ab\ell\Delta f$ and $E_1 = (1-\psi)ab\ell\Delta f$ still hold with $0 \leq \psi \leq 1$ and $0 \leq \ell' \leq \ell$.

At this point, a simple change of variable is introduced for convenience. Define $\lambda = 1-\xi$ with $0 \leq \lambda \leq 1$.

Now our approach would appear to have introduced another parameter λ in addition to ψ, but this is not the case. To see this, first observe that when $\Delta\phi_1$ is positive, the free energy of fusion which can be apportioned is $ab\ell\Delta f$, the amount in fact apportioned is $\psi ab\ell\Delta f$, and the fraction of the free energy of fusion which can be apportioned that is in fact apportioned is ψ. When $\Delta\phi_1$ is negative, the free energy of fusion which can be apportioned is $ab\ell\Delta f - (-\Delta\phi_1) = 2ab\sigma_e' + 2b\ell\sigma$, the amount in fact apportioned is $\lambda(2ab\sigma_e' + 2b\ell\sigma)$, and the fraction of the free energy of fusion which can be apportioned that is in fact apportioned is λ. If we always choose the same value for λ and ψ, then over the whole range of values for $\Delta\phi_1$, the fraction of the free energy of fusion which can be apportioned that is in fact apportioned has the same value. Let γ denote any particular value which is chosen for both ψ and λ, where $0 \leq \gamma \leq 1$.

As will be seen, the symbol γ has been introduced for clarity. Recall that $\psi = \frac{\ell'}{\ell}$, but an expression for λ in terms of ℓ' or vice versa still needs to be obtained, and furthermore, equal values of ψ and λ do <u>not</u> in general imply the same value of ℓ'. In our approach, then, ℓ' depends at least on the sign of $\Delta\phi_1$, but nevertheless, our approach has only one parameter, γ--the fraction of the free energy of fusion which can be apportioned that is in fact apportioned--which is a constant over the whole range of values for $\Delta\phi_1$.

In summary, the barriers in terms of the apportionment parameter γ are

$$\left.\begin{aligned} \Delta\phi_1 + E_1 &= (1-\gamma)(2ab\sigma'_e + 2b\ell\sigma) \\ E_1 &= ab\ell\Delta f - \gamma(2ab\sigma'_e + 2b\ell\sigma) \end{aligned}\right\} \text{ for } \Delta\phi_1 \le 0$$

$$\left.\begin{aligned} \Delta\phi_1 + E_1 &= 2ab\sigma'_e + 2b\ell\sigma - \gamma ab\ell\Delta f \\ E_1 &= (1-\gamma)ab\ell\Delta f \end{aligned}\right\} \text{ for } \Delta\phi_1 \ge 0$$

where we now observe that $(1-\gamma)(2ab\sigma'_e + 2b\ell\sigma) = 2ab\sigma'_e + 2b\ell\sigma - \gamma ab\ell\Delta f$ when $\Delta\phi_1 = 0$, i.e. $\Delta\phi_1 + E_1$ is a continuous function of ℓ and Δf at the points $(\ell,\Delta f)$ for which $\Delta\phi_1 = 0$. Note that the greater the value of the apportionment parameter γ, the smaller the value of both $\Delta\phi_1 + E_1$ and E_1.

Next, an expression for ℓ' in terms of λ is to be derived. Given $\Delta\phi_1 + E_1 = (1-\lambda)(2ab\sigma'_e + 2b\ell\sigma)$ for $\Delta\phi_1 < 0$, one can first find ψ <u>when $\Delta\phi_1 < 0$ holds</u> in terms of λ by equating the expressions

$$(1-\lambda)(2ab\sigma'_e + 2b\ell\sigma) = 2ab\sigma'_e + 2b\ell\sigma - \psi ab\ell\Delta f$$

whence

$$\psi = \lambda\left(\frac{2\sigma'_e}{\ell\Delta f} + \frac{2\sigma}{a\Delta f}\right) .$$

Clearly, equating these expressions and expressing ψ when $\Delta\phi_1 < 0$ in terms of λ is valid since decreasing $2ab\sigma'_e + 2b\ell\sigma$ by an amount $\psi ab\ell\Delta f$ must be equivalent to decreasing $2ab\sigma'_e + 2b\ell\sigma$ by $\lambda(2ab\sigma'_e + 2b\ell\sigma)$. Note that the expression $\left(\frac{2\sigma'_e}{\ell\Delta f} + \frac{2\sigma}{a\Delta f}\right)$ is always less than one when $\Delta\phi_1$ is negative. (To see this, simply observe that $\Delta\phi_1 < 0$ implies $2ab\sigma'_e + 2b\ell\sigma < ab\ell\Delta f$, and then divide both sides of this inequality by $ab\ell\Delta f$.) But $\psi = \frac{\ell'}{\ell}$ for all values of $\Delta\phi_1$ so that

$$\ell' = \lambda\ell\left(\frac{2\sigma'_e}{\ell\Delta f} + \frac{2\sigma}{a\Delta f}\right) .$$

Note that since λ cannot exceed one, the largest possible value of ℓ', i.e. the upper limit on ℓ', is $\ell\left(\frac{2\sigma'_e}{\ell\Delta f} + \frac{2\sigma}{a\Delta f}\right)$ for $\Delta\phi_1 < 0$; as mentioned previously, this upper limit is indeed less that ℓ for $\Delta\phi_1 < 0$.

For completeness, one can also find λ when $\Delta\phi_1 > 0$ holds in terms of ψ by equating the expressions

$$(1-\lambda)(2ab\sigma'_e + 2b\ell\sigma) = 2ab\sigma'_e + 2b\ell\sigma - \psi ab\ell\Delta f$$

whence

$$\lambda = \frac{\psi}{\left(\frac{2\sigma'_e}{\ell\Delta f} + \frac{2\sigma}{a\Delta f}\right)}$$

Clearly, equating these expressions and expressing λ when $\Delta\phi_1 > 0$ in terms of ψ is valid since decreasing $2ab\sigma'_e + 2b\ell\sigma$ by an amount $\psi ab\ell\Delta f$ must be equivalent to decreasing $2ab\sigma'_e + 2b\ell\sigma$ by $\lambda(2ab\sigma'_e + 2b\ell\sigma)$. Here again, $\psi = \frac{\ell'}{\ell}$. Note that $\left(\frac{2\sigma'_e}{\ell\Delta f} + \frac{2\sigma}{a\Delta f}\right)$ is always greater than one when $\Delta\phi_1$ is positive.

In summary, then, for $\Delta\phi_1 \leq 0$, one chooses a value from zero to one for the parameter γ, whence $\lambda = \gamma$, and then calculates $\psi = \lambda\left(\frac{2\sigma'_e}{\ell\Delta f} + \frac{2\sigma}{a\Delta f}\right)$. For $\Delta\phi_1 \geq 0$, one chooses a value from zero to one for the parameter γ, whence $\psi = \gamma$, and then calculates $\lambda = \frac{\psi}{\left(\frac{2\sigma'_e}{\ell\Delta f} + \frac{2\sigma}{a\Delta f}\right)}$. For all $\Delta\phi_1$, $\psi = \frac{\ell'}{\ell}$. Thus,

$$\left.\begin{aligned} \lambda &= \gamma \\ \psi &= \lambda\left(\frac{2\sigma'_e}{\ell\Delta f} + \frac{2\sigma}{a\Delta f}\right) \end{aligned}\right\} \text{ for } \Delta\phi_1 \leq 0$$

$$\left.\begin{aligned} &\psi = \gamma \\ &\lambda = \frac{\psi}{\left(\frac{2\sigma'_e}{\ell\Delta f} + \frac{2\sigma}{a\Delta f}\right)} \end{aligned}\right\} \text{ for } \Delta\phi_1 \geq 0$$

Incidentally, the constraint $2ab\sigma'_e + 2b\ell\sigma - \psi ab\ell\Delta f \geq 0$ combined with $0 \leq \psi \leq 1$ implies that the inequality

$$0 \leq \psi \leq 1 \text{ the smaller of 1 and } \left(\frac{2\sigma'_e}{\ell\Delta f} + \frac{2\sigma}{a\Delta f}\right)$$

must be satisfied, and clearly our theory has satisfied it.

Similarly, the constraint $ab\ell\Delta f - \lambda(2ab\sigma'_e + 2b\ell\sigma) \geq 0$ combined with $0 \leq \lambda \leq 1$ implies that the inequality

$$0 \leq \lambda \leq \text{ the smaller of 1 and } \frac{1}{\left(\frac{2\sigma'_e}{\ell\Delta f} + \frac{2\sigma}{a\Delta f}\right)}$$

must be satisfied, and clearly our theory has satisfied it.

The approach developed above can readily be applied to incorporate into the model the constraint that E_2 be nonnegative. Here, $E_2 = 2ab\sigma_e - \hat{\psi} ab\ell\Delta f$ can be negative when E is positive, and E is always positive (except when $\ell = 2\sigma_e/\Delta f$, which gives $E = 0$). The requirement $E_2 \geq 0$ implies that one is not allowed to apportion all of the free energy of fusion $ab\ell\Delta f$. If the amount $\hat{\psi} ab\ell\Delta f$ which is apportioned were to exceed $2ab\sigma_e$, then E_2 would be negative. Therefore, one has $E_2 = \eta 2ab\sigma_e$ where η is an apportionment parameter with $0 \leq \eta \leq 1$. And $E+E_2 = -2ab\sigma_e + ab\ell\Delta f + \eta 2ab\sigma_e = ab\ell\Delta f - (1-\eta)2ab\sigma_e$. For convenience, make the change of variable $\theta = 1-\eta$ with $0 \leq \theta \leq 1$ so that for all ℓ and Δf

$$E_2 = (1-\theta)2ab\sigma_e \quad \text{and} \quad E + E_2 = ab\ell\Delta f - \theta 2ab\sigma_e.$$

Observe that the barrier $E + E_2$ to the destruction of the second and each subsequent stem cannot be smaller than the free energy increase E that occurs upon its destruction, which implies that an adsorbed second or subsequent stem cannot completely crystallize before the barrier to the formation of that stem is surmounted, i.e. that the upper limit, determined below, on ℓ'' is less than ℓ.

Given $E_2 = (1-\theta)2ab\sigma_e$, one can find $\hat{\psi}$ in terms of θ by equating the expressions

$$(1-\theta)2ab\sigma_e = 2ab\sigma_e - \hat{\psi}ab\ell\Delta f$$

whence

$$\hat{\psi} = \theta \frac{2\sigma_e}{\ell\Delta f} .$$

Clearly, equating these expressions and expressing $\hat{\psi}$ in terms of θ is valid since decreasing E_2 with $\hat{\psi} = 0$ by an amount $\hat{\psi}ab\ell\Delta f$ must be equivalent to decreasing it by $\theta 2ab\sigma_e$. Note that the constraint $2ab\sigma_e - \hat{\psi}ab\ell\Delta f \geq 0$ implies that the inequality $0 \leq \hat{\psi} \leq \frac{2\sigma_e}{\ell\Delta f}$ must be satisfied; since $0 \leq \theta \leq 1$ holds, we have indeed satisfied this inequality. Also note that $\frac{2\sigma_e}{\ell\Delta f}$ is always less than or equal to one since $\ell \geq \frac{2\sigma_e}{\Delta f}$ has been established. (Incidentally, $2ab\sigma_e - \hat{\psi}ab\ell\Delta f \geq 0$ does <u>not</u> imply constraints $\ell \leq \frac{2\sigma_e}{\hat{\psi}\Delta f}$, $\Delta f \leq \frac{2\sigma_e}{\hat{\psi}\ell}$, or $\sigma_e \geq \frac{\hat{\psi}\ell\Delta f}{2}$.) Finally, recalling that $\hat{\psi} = \frac{\ell''}{\ell}$ and substituting above gives $\ell'' = \theta\frac{2\sigma_e}{\Delta f}$.

In the special case $\gamma = \theta = 0$, our model reduces to the case $\psi = \hat{\psi} = 0$ of the LH model which permits negative barriers for nonzero ψ.

VI. DETERMINATION OF THE SIGN OF $\Delta\phi_1$

At this point, one needs to determine when $\Delta\phi_1$ is positive, zero, and negative. Now $\Delta\phi_1 = 2ab\sigma'_e + 2b\ell\sigma - ab\ell\Delta f \geq 0$ implies $b\ell(2\sigma - a\Delta f) \geq -2ab\sigma'_e$; and there are three cases to consider.

Case (a): $2\sigma - a\Delta f > 0$ or $\Delta f < \frac{2\sigma}{a}$. Then the inequality $\ell > \frac{-2ab\sigma'_e}{b(2\sigma - a\Delta f)}$ is always satisfied since ℓ is always greater than zero, and hence $\Delta\phi_1 > 0$ holds.

Case (b): $2\sigma - a\Delta f = 0$ or $\Delta f = \frac{2\sigma}{a}$. Then $\Delta\phi_1 = 2ab\sigma'_e$, which is always positive or zero depending on σ'_e.

Thus, combining cases (a) and (b), we have $\Delta\phi_1 \geq 0$ for all ℓ when $\Delta f \leq \frac{2\sigma}{a}$. (So far, $\Delta\phi_1$ is zero only if both $\sigma'_e = 0$ and $\Delta f = \frac{2\sigma}{a}$.)

Case (c): $2\sigma - a\Delta f < 0$ or $\Delta f > \frac{2\sigma}{a}$. Then $\Delta\phi_1 \geq 0$ implies $-b\ell(a\Delta f - 2\sigma) \geq -2ab\sigma'_e$ or $\ell \leq \dfrac{\frac{2\sigma'_e}{\Delta f}}{1 - \frac{2\sigma}{a\Delta f}} = \ell_0$. Thus, when $\Delta f > \frac{2\sigma}{a}$, $\Delta\phi_1 \geq 0$ holds for $\ell \leq \ell_0$, and $\Delta\phi_1 \leq 0$ holds for $\ell \geq \ell_0$. (Observe that as $\Delta f \to \frac{2\sigma}{a}$ from values greater than $\frac{2\sigma}{a}$, $\ell_0 \to \infty$.) There is, however, one further condition to consider here. Recall that $\ell \geq \frac{2\sigma_e}{\Delta f}$ has been established. If $\ell_0 < \frac{2\sigma_e}{\Delta f}$ holds, then $\ell > \ell_0$ holds and consequently $\Delta\phi_1 < 0$ would hold for all ℓ. To determine when $\ell_0 < \frac{2\sigma_e}{\Delta f}$ holds, simply write $\dfrac{\frac{2\sigma'_e}{\Delta f}}{1 - \frac{2\sigma}{a\Delta f}} < \frac{2\sigma_e}{\Delta f}$, and noting that $\frac{2\sigma}{a\Delta f} < 1$, rearrange this inequality to get $\frac{2\sigma}{a\Delta f} < \frac{\sigma_e - \sigma'_e}{\sigma_e}$. Now, if $\sigma_e \leq \sigma'_e$, this inequality would be $\frac{2\sigma}{a\Delta f} < 0$, which is never satisfied; hence $\ell_0 < \frac{2\sigma_e}{\Delta f}$ never occurs when $\sigma_e \leq \sigma'_e$. If $\sigma_e > \sigma'_e$, $\ell_0 < \frac{2\sigma_e}{\Delta f}$ occurs when $\Delta f > \frac{2\sigma}{a}\left(\frac{\sigma_e}{\sigma_e - \sigma'_e}\right)$. Thus, if $\sigma_e > \sigma'_e$ and $\frac{2\sigma}{a} < \Delta f \leq \frac{2\sigma}{a}\left(\frac{\sigma_e}{\sigma_e - \sigma'_e}\right)$, $\Delta\phi_1 \geq 0$ holds for $\ell \leq \ell_0$ and $\Delta\phi_1 \leq 0$ holds for $\ell \geq \ell_0$, but for $\Delta f > \frac{2\sigma}{a}\left(\frac{\sigma_e}{\sigma_e - \sigma'_e}\right)$, $\Delta\phi_1 < 0$ holds for all ℓ.

VII. EXPRESSIONS FOR S_{Total} (T) AND ℓ(T)

If $\sigma_e \leq \sigma'_e$, our model with no negative barriers has

(1) $\Delta\phi_1 + E_1 = 2ab\sigma'_e + 2b\ell\sigma - \gamma ab\ell\Delta f$ for $\Delta f \leq \frac{2\sigma}{a}$

(2) $\Delta\phi_1 + E_1 = 2ab\sigma'_e + 2b\ell\sigma - \gamma ab\ell\Delta f$ for $\Delta f > \frac{2\sigma}{a}$ and $\ell \leq \ell_0$

(2) $\Delta\phi_1 + E_1 = (1-\gamma)(2ab\sigma'_e + 2b\ell\sigma)$ for $\Delta f > \frac{2\sigma}{a}$ and $\ell \geq \ell_0$

and if $\sigma_e > \sigma'_e$,

(1) $\Delta\phi_1+E_1 = 2ab\sigma'_e+2b\ell\sigma-\gamma ab\ell\Delta f$ for $\Delta f \le \frac{2\sigma}{a}$

(2) $\Delta\phi_1+E_1 = 2ab\sigma'_e+2b\ell\sigma-\gamma ab\ell\Delta f$ for $\frac{2\sigma}{a} < \Delta f \le \frac{2\sigma}{a}\left(\frac{\sigma_e}{\sigma_e-\sigma'_e}\right)$ and $\ell\le\ell_0$

(2) $\Delta\phi_1+E_1 = (1-\gamma)(2ab\sigma'_e+2b\ell\sigma)$ for $\frac{2\sigma}{a} < \Delta f \le \frac{2\sigma}{a}\left(\frac{\sigma_e}{\sigma_e-\sigma'_e}\right)$ and $\ell\ge\ell_0$

(3) $\Delta\phi_1+E_1 = (1-\gamma)(2ab\sigma'_e+2b\ell\sigma)$ for $\Delta f > \frac{2\sigma}{a}\left(\frac{\sigma_e}{\sigma_e-\sigma'_e}\right)$.

The purpose of categories (1), (2), and (3) will be seen shortly.

When $\Delta\phi_1+E_1 = 2ab\sigma'_e + 2b\ell\sigma - \gamma ab\ell\Delta f$, $E_1 = (1-\gamma)ab\ell\Delta f$, which we call Case I.

When $\Delta\phi_1+E_1 = (1-\gamma)(2ab\sigma'_e + 2b\ell\sigma)$, $E_1 = ab\ell\Delta f - \gamma(2ab\sigma'_e + 2b\ell\sigma)$, which we call Case II.

One always has

$$E_2 = (1-\theta)2ab\sigma_e$$

$$E+E_2 = -2ab\sigma_e + ab\ell\Delta f + E_2 = ab\ell\Delta f - \theta 2ab\sigma_e \ .$$

Also,

$$S(\ell,T) = \frac{N_0A_0(1-\frac{B}{A})}{1-\frac{B}{A}+\frac{B_1}{A}}$$

where $\frac{B}{A} = e^{-E/kT}$, $\frac{B_1}{A} = e^{-(E_1-E_2)/kT}$, and $A_0 = \beta\, e^{-(\Delta\phi_1+E_1)/kT}$.

Abbreviate $c' = \frac{2ab\sigma'_e}{kT}$, $c = \frac{2ab\sigma_e}{kT}$, $\alpha = \frac{2\sigma}{a\Delta f}$, and recall $\ell_1 = \frac{2\sigma_e}{\Delta f}$. Then $\frac{c}{\ell_1} = \frac{ab\Delta f}{kT}$, $\frac{\alpha c}{\ell_1} = \frac{2b\sigma}{kT}$, and $\frac{E}{kT} = -c + \frac{c}{\ell_1}\ell$. For Case I,

$$\frac{\Delta\phi_1+E_1}{kT} = \frac{2ab\sigma'_e}{kT} + \frac{2b\ell\sigma}{kT} - \frac{\gamma ab\ell\Delta f}{kT} = c' + \frac{c}{\ell_1}(\alpha-\gamma)\ell$$

$$\frac{E_1-E_2}{kT} = \frac{(1-\gamma)ab\ell\Delta f}{kT} - \frac{(1-\theta)2ab\sigma_e}{kT} = \frac{c}{\ell_1}(1-\gamma)\ell - (1-\theta)c$$

For Case II,

$$\frac{\Delta\phi_1+E_1}{kT} = \frac{(1-\gamma)(2ab\sigma_e'+2b\ell\sigma)}{kT} = (1-\gamma)c' + \frac{\alpha c}{\ell_1}(1-\gamma)\ell$$

$$\frac{E_1-E_2}{kT} = \frac{ab\ell\Delta f-\gamma(2ab\sigma_e'+2b\ell\sigma)}{kT} - \frac{(1-\theta)2ab\sigma_e}{kT} = \frac{c}{\ell_1}(1-\alpha\gamma)\ell-\gamma c'-(1-\theta)c$$

For Case I,

$$S_I(\ell,T) = \frac{\beta N_0 e^{-c'}\ e^{-(\alpha-\gamma)c\ell/\ell_1}\ (1-e^c\ e^{-c\ell/\ell_1})}{1-e^c\ e^{-c\ell/\ell_1} + e^{(1-\theta)c}\ e^{-(1-\gamma)c\ell/\ell_1}}$$

For Case II,

$$S_{II}(\ell,T) = \frac{\beta N_0 e^{-(1-\gamma)c'}\ e^{-(1-\gamma)\alpha c\ell/\ell_1}\ (1-e^c e^{-c\ell/\ell_1})}{1-e^c e^{-c\ell/\ell_1} + e^{(1-\theta)c} e^{\gamma c'}\ e^{-(1-\alpha\gamma)c\ell/\ell_1}}$$

For any Δf in category (1), then,

$$S^{(1)}_{Total}(T) = \frac{1}{\ell_u}\int_{\ell_1}^{\infty} S_I(\ell,T)\,d\ell \quad \text{and} \quad \bar{\ell}^{(1)}(T) = \frac{\int_{\ell_1}^{\infty}\ell\ S_I(\ell,T)d\ell}{\int_{\ell_1}^{\infty}S_I(\ell,T)d\ell}$$

For any Δf in category (2),

$$S^{(2)}_{Total}(T) = \frac{1}{\ell_u}\int_{\ell_1}^{\ell_0} S_I(\ell,T)d\ell + \frac{1}{\ell_u}\int_{\ell_0}^{\infty} S_{II}(\ell,T)\,d\ell$$

and

$$\bar{\ell}^{(2)}(T) = \frac{\int_{\ell_1}^{\ell_0}\ell S_I(\ell,T)d\ell + \int_{\ell_0}^{\infty}\ell\ S_{II}(\ell,T)d\ell}{\int_{\ell_1}^{\ell_0} S_I(\ell,T)d\ell + \int_{\ell_0}^{\infty}S_{II}(\ell,T)d\ell}$$

For any Δf in category (3),

$$S^{(3)}_{Total}(T) = \frac{1}{\ell_u}\int_{\ell_1}^{\infty}S_{II}(\ell,T)d\ell \quad \text{and} \quad \bar{\ell}^{(3)}(T) = \frac{\int_{\ell_1}^{\infty}\ell S_{II}(\ell,T)d\ell}{\int_{\ell_1}^{\infty}S_{II}(\ell,T)d\ell}$$

For purposes of comparison, the LH model which permits negative barriers has, for all ℓ and Δf,

$$\Delta\phi_1+E_1 = 2ab\sigma_e' + 2b\ell\sigma - \psi ab\ell\Delta f \quad \text{and} \quad E_2 = 2ab\sigma_e - \phi ab\ell\Delta f$$

so that

$$\frac{E_1 - E_2}{kT} = (1-\psi+\hat{\phi})\, \frac{c}{\ell_1}\, \ell - c$$

and

$$S^{(LH)}(\ell,T) = \frac{\beta N_0\, e^{-c'} e^{-c(\alpha-\psi)\ell/\ell_1}\, (1-e^{c} e^{-c\ell/\ell_1})}{1-e^{c}\, e^{-c\ell/\ell_1} + e^{c}\, e^{-(1-\psi+\hat{\phi})c\ell/\ell_1}}$$

and

$$S^{(LH)}_{Total}(\ell,T) = \frac{1}{\ell_u} \int_{\ell_1}^{\infty} S^{(LH)}(\ell,T)d\ell \quad \text{and} \quad \bar{\ell}^{(LH)}(T) = \frac{\int_{\ell_1}^{\infty} \ell S^{(LH)}(\ell,T)d\ell}{\int_{\ell_1}^{\infty} S^{(LH)}(\ell,T)d\ell}$$

As is the case in the LH model, our model has two parameters. The most logical choice for θ is $\theta = \gamma$; however, even with $\theta = \gamma$, our integrals cannot be evaluated analytically. There seems to be no special case (other than $\theta = \gamma = 0$) for which they could be evaluated analytically. At this point then, we proceed without setting $\theta = \gamma$.

VIII. EVALUATION OF THE $S_{Total}(T)$ AND $\bar{\ell}(T)$--THE VARIABLE TRANSFORMATIONS FOR THE NUMERICAL INTEGRATIONS

The required numerical integrations were easily performed interactively on the VAX using the IMSL subroutine DQDAGS.[5] Integrals to be evaluated using DQDAGS cannot have an infinite limit of integration. One way to proceed before using DQDAGS is to make a change of integration variable. Although DQDAGS can integrate functions with endpoints singularities (when the endpoints are finite), a change of variable which results in a transformed integrand which is bounded at all points including the finite endpoints in the new range of integration, is preferable to a change of variable which yields an improper integral albeit with finite integration limits. For each of the integrals appearing in $S^{(1)}_{Total}(T)$, $S^{(2)}_{Total}(T)$, and $S^{(3)}_{Total}(T)$, a variable transformation which resulted in a proper integral was in fact found. The same transformations did not transform the corresponding integrals in the numerators of $\ell^{(1)}(T)$, $\ell^{(2)}(T)$, and $\ell^{(3)}(T)$ into proper integrals; however, the transformed integrands were of the form $(-\ln x)f(x)$ with the singularity resulting only from the factor $\ln x$ as $x \to 0$. This endpoint singularity could be handled by DQDAGS.

Consider first the integral in $S^{(1)}_{Total}(T)$. The variable transformation consists of defining

$$x = e^{(1-\gamma)c}\, e^{-(1-\gamma)c\ell/\ell_1} .$$

Note that $x(\ell \to \infty) = 0$; the constant $e^{(1-\gamma)c}$, i.e. the ℓ-independent factor, is chosen so that $x(\ell = \ell_1) = 1$. Solving for ℓ in terms of x gives $\ell = \ell_1\left[1 - \frac{\ln x}{(1-\gamma)c}\right]$ provided $\gamma \neq 1$. Then $d\ell = -\frac{\ell_1}{(1-\gamma)c}\left(\frac{1}{x}\right)dx$. Furthermore, $e^{-(\alpha-\gamma)c\ell/\ell_1} = e^{-(\alpha-\gamma)c}\, x^{\frac{\alpha-\gamma}{1-\gamma}}$, $e^{-c\ell/\ell_1} = e^{-c}\, x^{\frac{1}{1-\gamma}}$, and $e^{-(1-\gamma)c\ell/\ell_1} = e^{-(1-\gamma)c}\, x$ so that

$$S^{(1)}_{Total}(T) = \frac{\beta N_0}{\ell_u}\, \frac{e^{-c'}e^{-(\alpha-\gamma)c}\ell_1}{(1-\gamma)c} \int_0^1 \frac{x^{\frac{\alpha-\gamma}{1-\gamma}}\left(1-x^{\frac{1}{1-\gamma}}\right)}{1-x^{\frac{1}{1-\gamma}} + e^{(1-\theta)c}\, e^{-(1-\gamma)c}\, x} \left(\frac{1}{x}\right) dx$$

Simplifying gives

$$S^{(1)}_{Total}(T) = \frac{\beta N_0}{\ell_u}\, \frac{e^{-c'}e^{-(\alpha-\gamma)c}\ell_1}{(1-\gamma)c} \int_0^1 \frac{x^{\frac{\alpha-1}{1-\gamma}}\left(1-x^{\frac{1}{1-\gamma}}\right)}{1-x^{\frac{1}{1-\gamma}} + e^{-(\theta-\gamma)c}\, x}\, dx$$

This is one of the integrals that was evaluated numerically by DQDAGS. Designate the integrand above as $f_1(x)$. Using the same variable transformation to evaluate the numerator of $\ell^{(1)}(T)$ gives

$$\ell^{(1)}(T) = \frac{\int_0^1 \ell_1\left[1-\frac{\ln x}{(1-\gamma)c}\right] f_1(x)\,dx}{\int_0^1 f_1(x)\, dx} = \ell_1 + \frac{\ell_1}{(1-\gamma)c}\, \frac{\int_0^1 (-\ln x) f_1(x)\,dx}{\int_0^1 f_1(x)\, dx}$$

Next, using the same transformation on the integral $\int_{\ell_1}^{\ell_0} S_I(\ell,T)\, d\ell$ appearing in $S^{(2)}_{Total}(T)$ gives

$$\int_{\ell_1}^{\ell_0} S_I(\ell,T)\,d\ell = \beta N_0 \frac{e^{-c'} e^{-(\alpha-\gamma)c} \ell_1}{(1-\gamma)c} \int_{x_0}^{1} f_1(x)\,dx$$

where

$$x_0 = x(\ell=\ell_0) = e^{(1-\gamma)c}\, e^{-(1-\gamma)c\ell_0/\ell_1} = e^{(1-\gamma)c}\, e^{-(1-\gamma)c'/(1-\alpha)}$$

with $\ell_0 = 2\sigma_e'/(1-\alpha)\Delta f$ as defined previously.

Similarly, the integral $\int_{\ell_1}^{\ell_0} \ell S_I(\ell,T)\,d\ell$ appearing in $\bar{\ell}^{(2)}(T)$ becomes

$$\int_{\ell_1}^{\ell_0} \ell S_I(\ell,T)\,d\ell = \frac{\beta N_0 e^{-c'} e^{-(\alpha-\gamma)c}\, \ell_1}{(1-\gamma)c} \left\{ \ell_1 \int_{x_0}^{1} f_1(x)\,dx + \frac{\ell_1}{(1-\gamma)c} \int_0^1 (-\ln x) f_1(x)\,dx \right\}$$

A different transformation is made on the integral $\int_{\ell_0}^{\infty} S_{II}(\ell,T)\,d\ell$ also appearing in $S_{Total}^{(2)}(T)$. Here, define

$$x = e^{(1-\gamma)(c-c')}\, e^{-(1-\gamma)\alpha c\ell/\ell_1} \quad .$$

Again $x(\ell \to \infty) = 0$; the constant $e^{(1-\gamma)(c-c')}$ is chosen so that $x(\ell=\ell_0) = x_0$, which is given above. Solving for ℓ gives $\ell = \frac{\ell_1}{\alpha c}\left[c-c' - \frac{\ln x}{(1-\gamma)}\right]$ provided $\gamma \neq 1$. Then $d\ell = -\frac{\ell_1}{(1-\gamma)\alpha c}\left(\frac{1}{x}\right) dx$. Furthermore, $e^{-(1-\gamma)\alpha c\ell/\ell_1} = e^{-(1-\gamma)(c-c')}\, x$,

$e^{-c\ell/\ell_1} = e^{-(c-c')/\alpha}\, x^{\frac{1}{(1-\gamma)\alpha}}$, and $e^{-(1-\alpha\gamma)c\ell/\ell_1} = e^{\frac{-(c-c')(1-\alpha\gamma)}{\alpha}}\, x^{\frac{1-\alpha\gamma}{(1-\gamma)\alpha}}$.

Substituting gives

$$\int_{\ell_0}^{\infty} S_{II}(\ell,T)\,d\ell = \frac{\beta N_0 e^{-(1-\gamma)c'} e^{-(1-\gamma)(c-c')} \ell_1}{(1-\gamma)\alpha c}$$

$$\cdot \int_0^{x_0} \frac{x\left[1 - e^{c} e^{-\left(\frac{c-c'}{\alpha}\right)} x^{\frac{1}{(1-\gamma)\alpha}}\right]}{1 - e^{c}\, e^{-\left(\frac{c-c'}{\alpha}\right)} x^{\frac{1}{(1-\gamma)\alpha}} + e^{(1-\theta)c}\, e^{\gamma c'}\, e^{-\left(\frac{c-c'}{\alpha}\right)(1-\alpha\gamma)} x^{\frac{1-\alpha\gamma}{(1-\gamma)\alpha}}} \left(\frac{1}{x}\right) dx$$

$$-\frac{\beta N_0\ e^{-(1-\gamma)c_{\ell_1}}}{(1-\gamma)\alpha c}\int_0^{x_0}\frac{1-e^c e^{-\left(\frac{c-c'}{\alpha}\right)}\ \frac{1}{x^{(1-\gamma)\alpha}}}{1-e^c e^{-\left(\frac{c-c'}{\alpha}\right)}\ \frac{1}{x^{(1-\gamma)\alpha}}+e^{-(\theta-\gamma)c}\ e^c\ e^{-\left(\frac{c-c'}{\alpha}\right)}\ \frac{1-\alpha\gamma}{x^{(1-\gamma)\alpha}}}\,dx$$

Designate the integrand above as $f_2(x)$. Thus,

$$S^{(2)}_{Total}(T)=\left(\frac{\beta N_0}{\ell_u}\ \frac{e^{-c'}e^{-(\alpha-\gamma)c_{\ell_1}}}{(1-\gamma)c}\int_{x_0}^{1}f_1(x)dx\right)+\left(\frac{\beta N_0}{\ell_u}\ \frac{e^{-(1-\gamma)c_{\ell_1}}}{(1-\gamma)\alpha c}\int_0^{x_0}f_2(x)dx\right)$$

Similarly, the integral $\int_{\ell_0}^{\infty}\ell S_{II}(\ell,T)d\ell$ appearing in $\ell^{(2)}(T)$ becomes

$$\int_{\ell_0}^{\infty}\ell S_{II}(\ell,T)d\ell=\frac{\beta N_0 e^{-(1-\gamma)c_{\ell_1}}}{(1-\gamma)\alpha c}\left\{\frac{(c-c')}{\alpha c}\ \ell_1\int_0^{x_0}f_2(x)dx+\frac{\ell_1}{(1-\gamma)\alpha c}\int_0^{x_0}(-\ln x)f_2(x)dx\right\}$$

Therefore,

$$\ell^{(2)}(T)=\frac{\left(\frac{1}{\beta N_0}\int_{\ell_1}^{\ell_0}\ell S_I(\ell,T)d\ell\right)+\left(\frac{1}{\beta N_0}\int_{\ell_0}^{\infty}\ell S_{II}(\ell,T)d\ell\right)}{\frac{\ell_u}{\beta N_0}\ S^{(2)}_{Total}(T)}$$

with the appropriate expressions for the integrals and $S^{(2)}_{Total}(T)$ to be substituted above.

Finally, consider the integral in $S^{(3)}_{Total}(T)$. The variable transformation to be made on this integral is

$$x=e^{(1-\gamma)\alpha c}\ e^{-(1-\gamma)\alpha c\ell/\ell_1}\ .$$

Again $x(\ell\to\infty)=0$ and the constant $e^{(1-\gamma)\alpha c}$ is chosen so that $x(\ell=\ell_1)=1$. Solving for ℓ gives $\ell=\ell_1\left[1-\frac{\ln x}{(1-\gamma)\alpha c}\right]$ provided $\gamma\neq1$. Then $d\ell=-\frac{\ell_1}{(1-\gamma)\alpha c}\left(\frac{1}{x}\right)dx$. Furthermore, $e^{-(1-\gamma)\alpha c\ell/\ell_1}=e^{-(1-\gamma)\alpha c}\ x$, $e^{-c\ell/\ell_1}=$

$e^{-c}\, x^{\frac{1}{(1-\gamma)\alpha}}$, and $e^{-(1-\alpha\gamma)c\ell/\ell_1} = e^{-(1-\alpha\gamma)c}\, x^{\frac{1-\alpha\gamma}{(1-\gamma)\alpha}}$ so that

$$S^{(3)}_{Total}(T) = \frac{\beta N_0}{\ell_u} \frac{e^{-(1-\gamma)(c'+\alpha c)}\ell_1}{(1-\gamma)\alpha c} \int_0^1 \frac{(1-x^{\frac{1}{(1-\gamma)\alpha}})}{1-x^{\frac{1}{(1-\gamma)\alpha}} + e^{-\theta c}\, e^{\gamma(c'+\alpha c)}\, x^{\frac{1-\alpha\gamma}{(1-\gamma)\alpha}}}\, dx$$

Designate the integrand above as $f_3(x)$. Using the same transformation to evaluate the numerator of $\ell^{(3)}(T)$ gives

$$\ell^{(3)}(T) = \ell_1 + \frac{\ell_1}{(1-\gamma)\alpha c} \frac{\int_0^1 (-\ln x) f_3(x)\,dx}{\int_0^1 f_3(x)\,dx}.$$

IX. RESULTS AND DISCUSSION

A VAX FORTRAN program was written to evaluate the required mathematical expressions. The program contains the statement CALL DQDAGS; and this IMSL subroutine performed the numerical integrations. All calculations were done double precision using the model parameter values given in Figure 3 of Reference 1; namely, $a = b = 5 \times 10^{-8}$ cm, $\sigma = 10$ erg/cm^2, $\sigma_e = 100$ erg/cm^2, $T_m^\circ = 500$ K, $\Delta h = 3 \times 10^9$ erg/cm^3, and $\Delta f = \Delta h(T_m^\circ - T)/T_m^\circ$. The average lamellar thickness calculated from the LH model is independent of σ_e'; this is true for our model only for $\Delta f \leq \frac{2\sigma}{a}$, however. Other quantities such as $S_{Total}(T)$ do depend on σ_e' even in the LH model, and physically,[6] one expects $0 \leq \sigma_e' \leq \sigma_e$. In the case $\sigma_e' = 0$, our model is slightly simpler, for then

$$\Delta\phi_1 + E_1 = 2b\ell\sigma - \gamma ab\ell\Delta f \qquad \Delta f \leq \frac{2\sigma}{a}$$

$$\Delta\phi_1 + E_1 = (1-\gamma)2b\ell\sigma \qquad \Delta f > \frac{2\sigma}{a}$$

Let us investigate our model in detail for the case $\sigma_e' = 0$ first; this is also the somewhat arbitrary choice for σ_e' made for the calculations[1,2] for the LH model.

Given the parameter values above and now with the choice $\theta = \gamma$, the calculated average lamellar thickness vs. temperature curves (ℓ vs T) are plotted in Figure 1 for the selected values of $\gamma = 0.0$, 0.50, 0.75, 0.90, and 0.95. Some of the data used to construct these plots is given in Table I. (For $\Delta f \leq \frac{2\sigma}{a}$, the average lamellar thickness is given by the expression for $\ell^{(1)}(T)$ given previously and for $\Delta f > \frac{2\sigma}{a}$, by the expression for $\ell^{(3)}(T)$ also given previously.) The effect of γ on ℓ as a function of T is readily apparent. For $\gamma = 0$ and $\gamma = \frac{1}{2}$, ℓ decreases monotonically with decreasing T, but for $\gamma = \frac{1}{2}$, there is indeed a break or discontinuity in the slope of ℓ vs. T, albeit barely discernible, at the temperature T* for which $\Delta f = \frac{2\sigma}{a}$, i.e. at $T = 433\frac{1}{3}$ K. (This statement will be qualified later.) As for $\gamma = \frac{1}{2}$, ℓ for $\gamma = \frac{3}{4}$, .9, and .95 decreases with decreasing T for all T for which $\Delta f > \frac{2\sigma}{a}$, and there is a break in the slope of ℓ vs T at $T = T^*$. Unlike for $\gamma = \frac{1}{2}$, the plotted ℓ vs T curves for $\gamma = \frac{3}{4}$, .9, and .95 pass through a relative minimum at a temperature for which $\Delta f < \frac{2\sigma}{a}$; the temperature T_* at which this relative minimum occurs appears to increase with increasing γ (for $\gamma = \frac{3}{4}$, it occurs between T = 440 and $433\frac{1}{3}$ K and so can hardly be seen on the plot). Also, over the interval $T < T_*$, ℓ vs T is at a relative maximum at $T = T^*$; and ℓ increases more rapidly as T approaches T* both from values greater and from values less than T* the larger the value of γ. Note that at least for all values of $\Delta f > \frac{2\sigma}{a}$, ℓ at a given T is larger the larger the value of γ.

For comparison, we have reproduced Figure 3(b) of Reference 1 as our Figure 2, which shows the LH model ℓ vs. T curves with $\hat{\psi} = \psi$ for the selected values of $\psi = 0, \frac{1}{4}, \frac{1}{3}, \frac{1}{2}, \frac{3}{4}$, .9, and .95. Some of the data which we calculated in order to construct these plots is given in Table II. The LH model $\psi = 0$ curve is identical to our $\gamma = 0$ curve. For $\Delta f \leq \frac{2\sigma}{a}$, each of the LH model "$\psi$ curves" is qualitatively similar but not quantitatively identical to its corresponding "γ curve" presented in Figure 1. Recall that the quantitative difference arises from the fact that the barrier E_2 has been constrained to be nonnegative, i.e. $E_2 = (1-\theta)2ab\sigma_e$. For $\Delta f > \frac{2\sigma}{a}$, however, the LH model ψ curves are in marked contrast to the γ curves; in particular, for each ψ curve, $\bar{\ell}$ approaches infinity asymptotically as Δf approaches $\frac{2\sigma}{\psi a}$. This is the behavior which is known as the $\delta\ell$ catastrophe. The above features of the LH curves for $\psi \leq .95$ also apply to LH curves for $.95 < \psi \leq 1$; calculations for the special case $\psi = 1$ can be done using the analytical expression obtained from $\bar{\ell}^{(LH)}(T)$ in the case $\hat{\psi} = \psi$. The curves for $.95 < \psi \leq 1$ are similar to the $\psi = .95$ curve; Figure 3(b) of Reference 1 gives a sketch of the $\psi = 1$ curve, which exhibits the $\delta\ell$ catastrophe at $\Delta f = \frac{2\sigma}{a}$.

By contrast, the γ curves for high values of γ less than one do not exhibit an infinite average lamellar thickness. Curves for $\gamma = 0.99$ and $\gamma = 0.998$ are presented in Figures 3 and 4, respectively, and do exhibit the features described previously for the $\gamma = \frac{3}{4}$, .9, and .95 curves. Again, for $\Delta f \leq \frac{2\sigma}{a}$, the curves for $\gamma = .99$ and $\gamma = .998$ are qualitatively very similar to LH curves with $\psi = .99$ and $\psi = .998$, respectively. Calculations for $\gamma > .998$ as well as for $\gamma = 1$ apparently cannot be done using the expressions for $\bar{\ell}^{(1)}(T)$ and $\bar{\ell}^{(3)}(T)$ as a result of the factor $(1-\gamma)$ appearing in various denominators.

One point is worth emphasizing here; namely, the relationship between γ and ψ. In both our model and the LH model, $\psi = \frac{\ell'}{\ell}$, but this ratio in the LH model is a constant, whereas in our model

$$\psi = \begin{cases} \gamma\left(\frac{2\sigma_e'}{\ell\Delta f} + \frac{2\sigma}{a\Delta f}\right) & \Delta\phi_1 \leq 0 \\ \\ \gamma & \Delta\phi_1 \geq 0 \end{cases} .$$

For the case $\sigma_e' = 0$, this becomes

$$\psi = \begin{cases} \gamma\,\frac{2\sigma}{a\Delta f} & \Delta f \geq \frac{2\sigma}{a} \\ \\ \gamma & \Delta f \leq \frac{2\sigma}{a} \end{cases} .$$

Now, for any given ψ, say ψ_j, ℓ in the LH model is infinite for all $\Delta f \geq \frac{2\sigma}{\psi_j a}$; and for all $\Delta f \geq \frac{2\sigma}{\psi_j a}$, there is no finite value of ℓ for any $\psi \geq \psi_j$. Equivalently, a value of $\psi \geq \psi_j$ is not possible for a chain-folded system for all $\Delta f \geq \frac{2\sigma}{\psi_j a}$, that is, high values of ψ do not lead to chain-folded polymer crystals at high enough supercooling according to the LH model. Experiment, however, gives chain-folded crystals at high supercooling with an average lamellar thickness that decreases monotonically with decreasing temperature. As we have seen, our one-parameter (i.e. γ) model with $\sigma_e' = 0$ does reproduce this high supercooling behavior. And yet, high values of ψ, i.e. of the ratio $\frac{\ell'}{\ell}$, are <u>not</u> associated with our high-supercooling chain-folded systems. To see this, first introduce the dimensionless quantity x, where $0 < x < 1$. Then for any $\Delta f = \frac{2\sigma}{xa}$, $\psi = \gamma \frac{2\sigma}{a\Delta f} = \gamma x$. Since γ cannot exceed one, ψ in our model cannot exceed x_j for any $\Delta f \geq \frac{2\sigma}{x_j a}$, where x_j is any given value of x. But this is exactly what was found for ψ in the LH model, i.e. that a value of ψ greater than or equal to ψ_j is not possible for any $\Delta f \geq \frac{2\sigma}{\psi_j a}$. Thus, for $\Delta f > \frac{2\sigma}{a}$, our model, through the imposition of the constraint that barriers be nonnegative, places exactly the same upper limit, $\frac{2\sigma}{a\Delta f}$, on our ψ that is predicted for ψ in the LH model. However, for $\Delta f > \frac{2\sigma}{a}$, our model, unlike the LH model, predicts ℓ vs. T in qualitative agreement with experiment for all values of our model parameter γ less than one.

Thus, the selected calculations done for our model indicate that, for the case $\sigma_e' = 0$, our model does <u>not</u> exhibit an infinite average lamellar thickness for any value of γ less than one. Most importantly, at least for all T for which $\Delta f > \frac{2\sigma}{a}$, our calculations indicate that our $\sigma_e' = 0$ model predicts ℓ vs. T curves which are monotonically decreasing with decreasing T in agreement with experiment. That is, we have successfully extended the LH model to highest supercooling. This success coupled with the numerical results shown in Figure 1 increases our confidence in using low values of γ such as $\gamma = 0$ as a first approximation for convenience in practice.[3] Our model curves do show an anomaly, i.e. a break-in slope, at $T = T^*$. We strongly suspect that there is indeed a break in slope at $T = T^*$ because the relation

$$\psi = \begin{cases} \gamma \dfrac{2\sigma}{a\Delta f} & \Delta f \geq \dfrac{2\sigma}{a} \\ \gamma & \Delta f \leq \dfrac{2\sigma}{a} \end{cases}$$

implies that $\frac{d\psi}{dT}$ is discontinuous at $\Delta f = \frac{2\sigma}{a}$; however, we have not yet evaluated $\frac{d\ell}{dT}$ at $\Delta f = \frac{2\sigma}{a}$. This anomaly is apparently negligible up to γ values of about $\frac{1}{2}$, where the slope of ℓ vs. T has the same sign (positive) regardless of whether the point $\Delta f = \frac{2\sigma}{a}$ is approached from values of Δf higher or lower than $\frac{2\sigma}{a}$. As γ increases, however, this anomaly becomes pronounced with the concomitant appearance of a relative maximum in ℓ at $T = T^*$ and a relative minimum in ℓ at $T = T_*$; necessarily then, the slope of ℓ vs. T as Δf approaches $\frac{2\sigma}{a}$ from values less than $\frac{2\sigma}{a}$ becomes negative. We will refer to this undesirable behavior, manifest at high values of γ, as the ℓ anomaly. Unlike the $\delta\ell$ catastrophe in the LH model, the relative maximum in ℓ vs. T, as noted above, always appears at $\Delta f = \frac{2\sigma}{a}$ for all values of γ given that $\sigma_e' = 0$. Despite the ℓ anomaly, we see that the exclusion of negative barriers--the only difference between our model and the LH model--has strengthened the Lauritzen-Hoffman approach to polymer crystallization.

One set of results with $\theta \neq \gamma$ is presented in Table III. Here, we see that for $\gamma = \frac{1}{2}$ and $\theta = 1$, the calculated $\ell(T)$ differ only slightly from the case with $\gamma = \frac{1}{2}$ and $\theta = \frac{1}{2}$.

Next, we investigated our model for $\sigma_e' \neq 0$. (Recall that ℓ for the LH model is independent of σ_e' and that our model is independent of σ_e' for $\Delta f \leq \frac{2\sigma}{a}$.) Using the same values for a, b, σ, σ_e, T_m°, and Δh as above and again with $\theta = \gamma$, ℓ vs. T curves for $\sigma_e' = 0$, 60, 100, and 150 erg/cm^2--each with $\gamma = \frac{1}{2}$--are plotted together in Figure 5. Some of the $\sigma_e' \neq 0$ data used to construct these plots is given in Tables IV and V (and the $\sigma_e' = 0$ data has been seen previously in Table I). From Figure 5, we see that ℓ vs. T is relatively insensitive to the value of σ_e' for $\gamma = \frac{1}{2}$. For $\sigma_e' = 0$, 60, and 100 erg/cm^2, ℓ decreases monotonically with decreasing T, although for $\sigma_e' = 100$ erg/cm^2, the ℓ vs. T curve is almost flat near T = 405 K. For $\sigma_e' =$ 150 erg/cm^2, there is a relative minimum in ℓ vs. T near T = 405 K, and the curve passes through a small and "diffuse" relative maximum at a lower temperature. Recall that one expects $0 \le \sigma_e' \le \sigma_e$ so that with $\sigma_e =$ 100 erg/cm^2, $\sigma_e' = 150$ erg/cm^2 may not be realistic but is examined in order to explore the model predictions as a function of σ_e'.

The ℓ vs. T curves for $\sigma_e' = 0$, 60, 100, and 150 erg/cm^2--each with $\gamma = \frac{3}{4}$--are presented in Figure 6. The curves pass through a common relative minimum between T = 440 and $433\frac{1}{3}$ K (for which $\Delta f < \frac{2\sigma}{a}$), and then each curve rises and passes through a relative maximum, that maximum being relatively higher and occurring at higher Δf the larger the value of σ_e'. At each maximum, there would appear to be a break in the slope of ℓ vs. T; the slope of ℓ vs. T as Δf approaches $\frac{2\sigma}{a}$ both from values greater and from values less than $\frac{2\sigma}{a}$ is greater in magnitude the larger the value of σ_e'. Having passed through its maximum, each curve decreases monotonically with decreasing T thereafter.

One should be careful to note that what appears to be a break in the slope of ℓ vs. T when $\sigma_e' \neq 0$ is probably not a break in slope; $\frac{d\ell^{(2)}(T)}{dT}$ should be continuous for all relevant T. Whether a break in the slope of ℓ vs. T occurs at $\Delta f = \frac{2\sigma}{a}$ when $\sigma_e' \neq 0$ as was presumed true for $\sigma_e' = 0$ cannot be determined conclusively from the appearance of the graphs, although the break appears to be absent.

Qualitatively similar ℓ vs. T curves are obtained for $\gamma = 0.9$ and $\sigma_e' = 0$, 60, 100 and 150 erg/cm^2 as is shown in Figure 7. Here, the relative maxima are higher and "sharper" than the corresponding $\gamma = \frac{3}{4}$ curves, and they have moved to higher temperature. For $\gamma = 0.99$, the analogous curves, shown in Figure 8, exhibit ℓ values which are unrealistically large as well as maxima which are extremely "sharp".

The relationship between γ and ψ with $\sigma_e' \neq 0$ is worth emphasizing at this point. To reiterate, in both our model and the LH model, $\psi = \frac{\ell'}{\ell}$, but this ratio in the LH model is a constant, whereas in our model

$$\psi(\ell,T) = \begin{cases} \gamma\left(\dfrac{2\sigma_e'}{\ell\Delta f} + \dfrac{2\sigma}{a\Delta f}\right) & \Delta\phi_1(\ell,T) \leq 0 \\ \gamma & \Delta\phi_1(\ell,T) \geq 0 \end{cases}$$

where the notation $\psi(\ell,T)$ and $\Delta\phi_1(\ell,T)$ emphasizes here the dependence of ψ and $\Delta\phi_1$ on ℓ and T. (The T dependence, of course, enters through Δf.) Recalling the conditions which govern the sign of $\Delta\phi_1$ then gives when $\sigma_e > \sigma_e'$

$$\psi(\ell,T) = \begin{cases} \gamma\left(\dfrac{2\sigma_e'}{\ell\Delta f} + \dfrac{2\sigma}{a\Delta f}\right) & \begin{cases} \text{for all } \ell \text{ when } \Delta f > \dfrac{2\sigma}{a}\left(\dfrac{\sigma_e}{\sigma_e - \sigma_e'}\right) \\ \text{for } \ell \geq \ell_0 \text{ when } \dfrac{2\sigma}{a} < \Delta f \leq \dfrac{2\sigma}{a}\left(\dfrac{\sigma_e}{\sigma_e - \sigma_e'}\right) \end{cases} \\[2em] \gamma & \begin{cases} \text{for } \ell \leq \ell_0 \text{ when } \dfrac{2\sigma}{a} < \Delta f \leq \dfrac{2\sigma}{a}\left(\dfrac{\sigma_e}{\sigma_e - \sigma_e'}\right) \\ \text{for all } \ell \text{ when } \Delta f \leq \dfrac{2\sigma}{a} \end{cases} \end{cases}$$

and when $\sigma_e \leq \sigma_e'$

$$\psi(\ell,T) = \begin{cases} \gamma\left(\dfrac{2\sigma_e'}{\ell\Delta f} + \dfrac{2\sigma}{a\Delta f}\right) & \text{for } \ell \geq \ell_0 \text{ when } \Delta f > \dfrac{2\sigma}{a} \\ \gamma & \begin{cases} \text{for } \ell \leq \ell_0 \text{ when } \Delta f > \dfrac{2\sigma}{a} \\ \text{for all } \ell \text{ when } \Delta f \leq \dfrac{2\sigma}{a} \end{cases} \end{cases}$$

where $\ell_0 = \dfrac{\dfrac{2\sigma_e'}{\Delta f}}{1 - \dfrac{2\sigma}{a\Delta f}}$. Now, on an ℓ vs. T curve, one has

$$\psi(\hat{\ell},T) = \begin{cases} \gamma\left(\frac{2\sigma_e'}{\hat{\ell}\Delta f} + \frac{2\sigma}{a\Delta f}\right) & \Delta\phi_1(\hat{\ell},T) \le 0 \\ \gamma & \Delta\phi_1(\hat{\ell},T) \ge 0 \end{cases}$$

where the conditions which govern the sign of $\Delta\phi_1(\hat{\ell},T)$ are those given above for $\Delta\phi_1(\ell,T)$ but with ℓ replaced by $\hat{\ell}$. Therefore, the temperature T_0 of a point $(\hat{\ell}_0, T_0)$ on an $\hat{\ell}$ vs. T curve and at which $\Delta\phi_1(\hat{\ell},T) = \Delta\phi_1(\hat{\ell}_0,T_0) = 0$ is the solution to the following non-linear algebraic equation in the one unknown T:

$$\hat{\ell}^{(2)}(T) = \ell_0$$

or

$$\frac{\int_{\ell_1}^{\ell_0} \ell S_I d\ell + \int_{\ell_0}^{\infty} \ell S_{II} d\ell}{\int_{\ell_1}^{\ell_0} S_I d\ell + \int_{\ell_0}^{\infty} S_{II} d\ell} = \frac{\frac{2\sigma_e'}{\Delta f}}{1 - \frac{2\sigma}{a\Delta f}}$$

If $\sigma_e > \sigma_e'$, T_0 will correspond to a value of Δf in the range $\frac{2\sigma}{a} < \Delta f \le \frac{2\sigma}{a}\left(\frac{\sigma_e}{\sigma_e - \sigma_e'}\right)$, but if $\sigma_e \le \sigma_e'$, T_0 will correspond to a value of Δf in the range $\Delta f > \frac{2\sigma}{a}$.

Rather than attempt to solve the above equation iteratively, one simply plots the left-hand side $\hat{\ell}^{(2)}(T)$ vs. T and the right-hand side $\ell_0(T)$ vs. T on the same graph, and T_0 is given by a point of intersection of the two curves. Note that as Δf approaches $\frac{2\sigma}{a}$ from values greater than $\frac{2\sigma}{a}$, ℓ_0 approaches infinity and that ℓ_0 decreases monotonically with decreasing T for $\Delta f > \frac{2\sigma}{a}$. For each of the $\hat{\ell}$ vs. T curves with $\sigma_e' \ne 0$ presented in Figures 5 through 8, we found one point of intersection $(\hat{\ell}_0, T_0)$, which is designated on each curve in the figures by an open circle. We also found that $\hat{\ell}^{(2)}(T) > \hat{\ell}_0$ holds when $T < T_0$ and that $\hat{\ell}^{(2)}(T) < \hat{\ell}_0$ holds when $T > T_0$. Thus, $\Delta\phi(\hat{\ell},T) < 0$ holds for $T < T_0$ and $\Delta\phi(\hat{\ell},T) > 0$ holds for $T > T_0$. Our final result is that, on an $\hat{\ell}$ vs. T curve,

$$\psi = \begin{cases} \gamma\left(\frac{2\sigma_e'}{\hat{\ell}\Delta f} + \frac{2\sigma}{a\Delta f}\right) & 0 < T \le T_0 \\ \gamma & T_0 \le T < T_m^\circ \end{cases}$$

Note that if the dimensionless quantity x, $0 < x < 1$, is again introduced by writing $\Delta f = \frac{2\sigma}{xa}$, $\psi = \gamma x\left(\frac{a\sigma_e'}{\ell\sigma} + 1\right)$ so that, unlike the case $\sigma_e' = 0$, ψ can exceed x_j for some $\Delta f \geq \frac{2\sigma}{x_j a}$, where x_j is any given value of x. Clearly, one can easily calculate ψ for each point on the $\sigma_e' \neq 0$ ℓ vs. T curves, but we have not yet done so.

Thus, from the graphs, we see that the ℓ anomaly becomes more pronounced but moves to higher temperature as γ increases for a fixed nonzero value of σ_e'. That is, although the relative maximum in ℓ vs. T can appear at some $\Delta f > \frac{2\sigma}{a}$ when σ_e' is nonzero, the maximum becomes less pronounced as it moves to lower temperature upon an increase in γ. Our model, then, does not fail at high supercooling, but does exhibit anomalous behavior for temperatures corresponding to values of Δf "just" greater and "just" less than $\frac{2\sigma}{a}$. This undesirable behavior is pronounced for large values of γ and is more pronounced for larger values of σ_e' for a given γ.

We can easily rationalize mathematically how our calculated ℓ vs. T curves can rise with decreasing T for some $\Delta f > \frac{2\sigma}{a}$ when σ_e' is nonzero. Recall that the expression for $\ell^{(2)}(T)$, namely

$$\ell^{(2)}(T) = \frac{\int_{\ell_1}^{\ell_0} \ell S_I(\ell,T)d\ell + \int_{\ell_0}^{\infty} \ell S_{II}(\ell,T)d\ell}{\int_{\ell_1}^{\ell_0} S_I(\ell,T)d\ell + \int_{\ell_0}^{\infty} S_{II}(\ell,T)d\ell}$$

contains two different integrands $S_I(\ell,T)$ and $S_{II}(\ell,T)$. Depending on σ_e', γ, and T, the contribution of the integrals involving $S_I(\ell,T)$ to $\ell^{(2)}(T)$ may outweigh the contribution of the integrals involving $S_{II}(\ell,T)$, and in some cases, our calculations show that to a very good approximation

$$\ell^{(2)}(T) \approx \frac{\int_{\ell_1}^{\ell_0} \ell S_I(\ell,T)d\ell}{\int_{\ell_1}^{\ell_0} S_I(\ell,T)d\ell} \quad \text{with } \ell_0 \text{ approaching infinity.}$$

But this is our expression for $\bar{\ell}^{(1)}(T)$ for the interval $\Delta f \le \frac{2\sigma}{a}$, and the results of our calculations using $\bar{\ell}^{(1)}(T)$ have been found to differ little from results using $\bar{\ell}^{(LH)}(T)$, i.e. the LH theory. Not unexpectedly then, $\bar{\ell}^{(2)}(T)$ can increase with decreasing T for some $\Delta f > \frac{2\sigma}{a}$. We note that the numerator of $S_I(\ell,T)$, like the numerator of $S^{(LH)}(\ell,T)$, contains the factor $A_0 = e^{-c'} e^{-b\ell(2\sigma-\gamma a\Delta f)/kT}$, the form of which has been associated with[7] increases in $\bar{\ell}$ with decreasing T.

X. CONCLUSIONS

Thus, the $\bar{\ell}$ anomaly is apparently connected to the expression $\Delta\phi_1 + E_1 - 2ab\sigma_e' + 2b\ell\sigma - \gamma ab\ell\Delta f$ even when the maximum in $\bar{\ell}$ vs. T occurs at a temperature for which Δf exceeds $\frac{2\sigma}{a}$. Our results with $\sigma_e' = 0$ clearly indicate that the $\bar{\ell}$ anomaly--and in part the $\delta\ell$ catastrophe of the LH theory--are associated with the interval $\Delta f \le \frac{2\sigma}{a}$ and are thus connected to the expression $\Delta\phi_1+E_1 - 2ab\sigma_e' + 2b\ell\sigma - \gamma ab\ell\Delta f$. Even when high values of γ or ψ are considered unrealistic as has been elucidated[3] recently, however, there is no guarantee that the LH theory as well as our extension of it has not failed to incorporate an as yet unknown constraint or feature which would improve the model results at high γ values. For example, high γ values may be unrealistic, but the $\bar{\ell}$ values for high γ from an improved model may simply be unrealistically large but nevertheless monotonically decreasing with decreasing T for all T. Further work along this line would probably be mostly of theoretical interest rather than essential for use in practice.

Although the $\bar{\ell}$ anomaly remains in our model, we have shown that the $\delta\ell$ catastrophe of the LH theory is in part related to the failure to exclude negative barriers. Furthermore, our model is successful, for it shows that the Lauritzen-Hoffman approach to polymer crystallization, subject to the exclusion of negative barriers, is consistent with experimental behavior at very high supercooling. We conclude that we can safely extend our version of the LH theory to treat systems interacting with an external electric field.

REFERENCES

I.1 H.L. Marand, R.S. Stein, and G.M. Stack, J. Polym. Sci. Polym. Phys. Ed. 26, 1361 (1988).

I.2 H.L. Marand and R.S. Stein, J. Polym. Sci. Polym. Phys. Ed. 27, 1089 (1989).

I.3 J.I. Scheinbeim, B.A. Newman, and A. Sen, Macromolecules 19, 1454 (1986).

1. J.I. Lauritzen, Jr. and J.D. Hoffman, J. Appl. Phys. 44, 4340 (1973).

2. J.D. Hoffman, G.T. Davis, and J.I. Lauritzen, Jr., in "Treatise on Solid State Chemistry", Vol. 3, N.B. Hannay, Ed., Plenum Press, New York, 1976, Chapter 7, pp. 497-614.

3. J.D. Hoffman and R.L. Miller, Macromolecules 22, 3038 (1989).

4. D. Turnbull and J.C. Fisher, J. Chem. Phys. 17, 71 (1949).

5. USER'S MANUAL-MATH/LIBRARY-FORTRAN Subroutines for Mathematical Applications, IMSL, Inc., 1987, Chapter 4, pp. 561-568.

6. J.D. Hoffman, L.J. Frolen, G.S. Ross, and J.I. Lauritzen, Jr., J. Res. Nat. Bur. Stand. 79A, 671 (1975).

7. I.C. Sanchez, J. Macromol. Sci. - Revs. Macromol. Chem. C10, 113-148 (1974).

FIGURE CAPTIONS

Figure 1. Plots of Average Lamellar Thickness vs. Temperature for $\gamma = 0$, $\frac{1}{2}$, $\frac{3}{4}$, 0.90, and 0.95, each with $\sigma_e' = 0$. See text for a, b, σ, σ_e, T_m°, and Δh which are the same for Figures 1 through 8. Figures 1 through 8 have $\theta = \gamma$.
At $T = 433\frac{1}{3}$ K (i.e. $\Delta f = \frac{2\sigma}{a}$), $\Delta\phi_1 = 0$.
For $T \geq 433\frac{1}{3}$ K, $\Delta\phi_1 \geq 0$ and $\psi = \gamma$.
For $T \leq 433\frac{1}{3}$ K, $\Delta\phi_1 \leq 0$ and $\psi = \gamma(\frac{2\sigma}{a\Delta f})$.

Figure 2. Plots of Average Lamellar Thickness vs. Temperature for $\psi = 0$, $\frac{1}{4}$, $\frac{1}{3}$, $\frac{1}{2}$, $\frac{3}{4}$, 0.90, and 0.95 reproduced from the Lauritzen-Hoffman Model (Reference 1); plots are independent of σ_e'.

Figure 3. Plot of Average Lamellar Thickness vs. Temperature for $\gamma = 0.99$ and $\sigma_e' = 0$. Again, for $T \geq 433\frac{1}{3}$ K, $\psi = \gamma$ and for $T \leq 433\frac{1}{3}$ K, $\psi = \gamma\left(\frac{2\sigma}{a\Delta f}\right)$.

Figure 4. Plot of Average Lamellar Thickness vs. Temperature for $\gamma = 0.998$ and $\sigma_e' = 0$. Again, for $T \geq 433\frac{1}{3}$ K, $\psi = \gamma$ and for $T \leq 433\frac{1}{3}$ K, $\left(\frac{2\sigma}{a\Delta f}\right)$.

Figure 5. Plots of Average Lamellar Thickness vs. Temperature for $\sigma_e' = 0$, 60, 100, and 150 ergs/cm^2, each with $\gamma = \frac{1}{2}$. Each open circle designates the point (ℓ_0, T_0) at which $\Delta\phi_1(\ell,T) = 0$. For $T \geq T_0$, $\Delta\phi_1 \geq 0$ and $\psi = \gamma$. For $T \leq T_0$, $\Delta\phi_1 \leq 0$ and $\psi = \gamma\left(\frac{2\sigma_e'}{\ell\Delta f} + \frac{2\sigma}{a\Delta f}\right)$.

Figure 6. Plots of Average Lamellar Thickness vs. Temperature for $\sigma_e' = 0$, 60, 100, and 150 ergs/cm^2, each with $\gamma = \frac{3}{4}$. Again, each open circle identifies the temperature T_0 (see Figure 5).

Figure 7. Plots of Average Lamellar Thickness vs. Temperature for $\sigma_e' = 0$, 60, 100, and 150 ergs/cm^2, each with $\gamma = 0.90$. Again,

each open circle identifies the temperature T_0 (see Figure 5).

Figure 8. Plots of Average Lamellar Thickness vs. Temperature for σ'_e = 0, 60, 100, and 150 ergs/cm^2, each with γ = 0.99. For σ'_e = 0, 60, 100, and 150 ergs/cm^2, T_0 = 433 $\frac{1}{3}$ K, 432.2 K, 432.1 K, and 432.0 K, respectively (see Figure 5).

TABLE CAPTIONS

Table I. Average Lamellar Thickness as a Function of Temperature for $\gamma = 0, \frac{1}{2}$, and 0.90, each with $\sigma_e' = 0$ and $\theta = \gamma$. See Figure 1.

Table II. Average Lamellar Thickness as a Function of Temperature for $\psi = \frac{1}{2}$ and 0.90 reproduced from the Lauritzen-Hoffman Model (Reference 1), each with $\hat{\psi} = \psi$ and independent of σ_e'. See Figure 2.

Table III. Average Lamellar Thickness as a Function of Temperature for $\gamma = \frac{1}{2}$, $\theta = 1$, and $\sigma_e' = 0$. See text for the usual values of a, b, σ, σ_e, T_m°, and Δh.

Table IV. Average Lamellar Thickness as a Function of Temperature for $\sigma_e' = 60$, 100, and 150 ergs/cm^2, each with $\gamma = \frac{1}{2}$. See Figure 5.

Table V. Average Lamellar Thickness as a Function of Temperature for $\sigma_e' = 60$, 100, and 150 ergs/cm^2, each with $\gamma = 0.90$. See Figure 7.

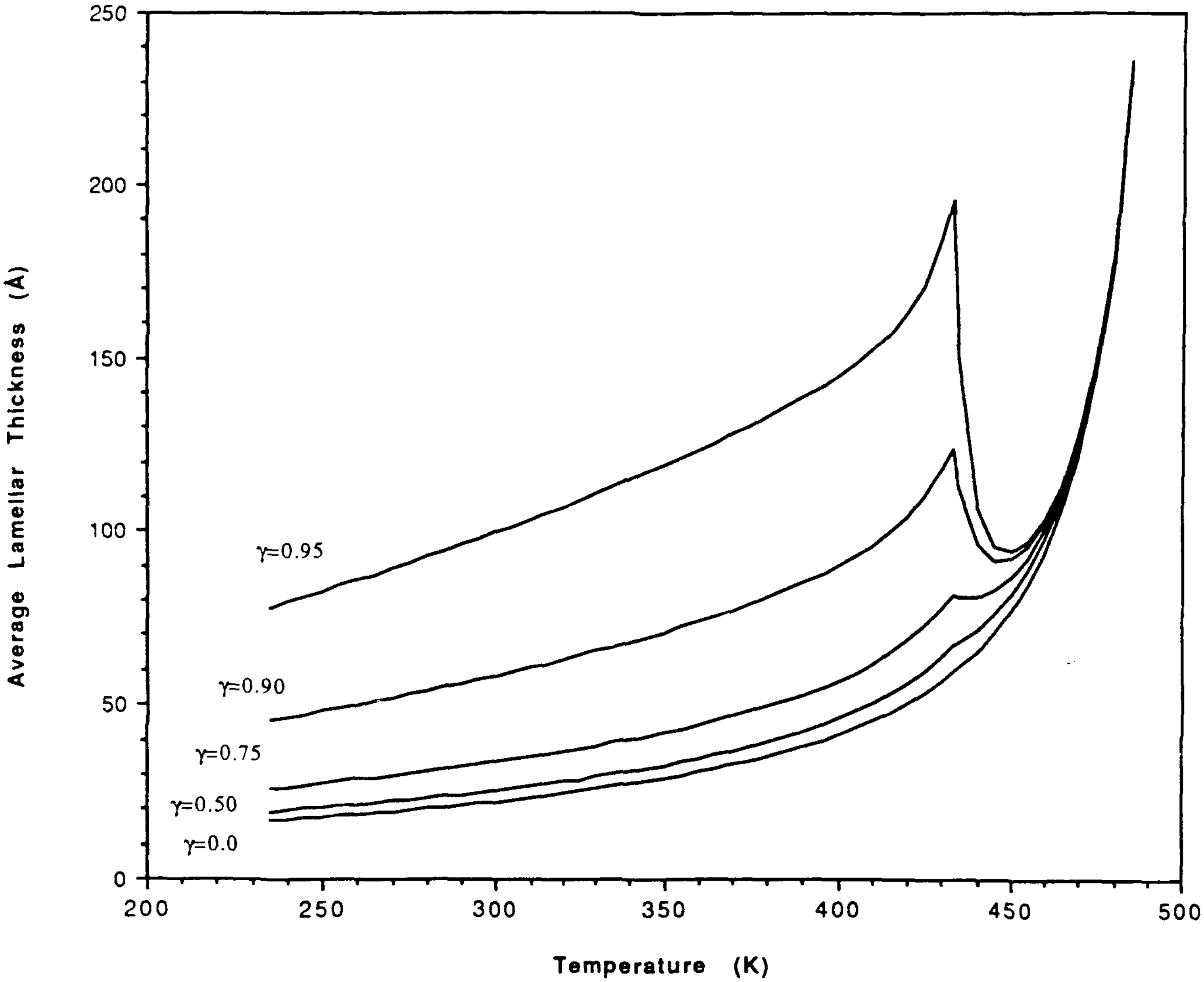

Average Lamellar Thickness (Å)
Temperature (K)
γ=0.95
γ=0.90
γ=0.75
γ=0.50
γ=0.0
0
50
100
150
200
250
200
250
300
350
400
450
500

Figure 1.

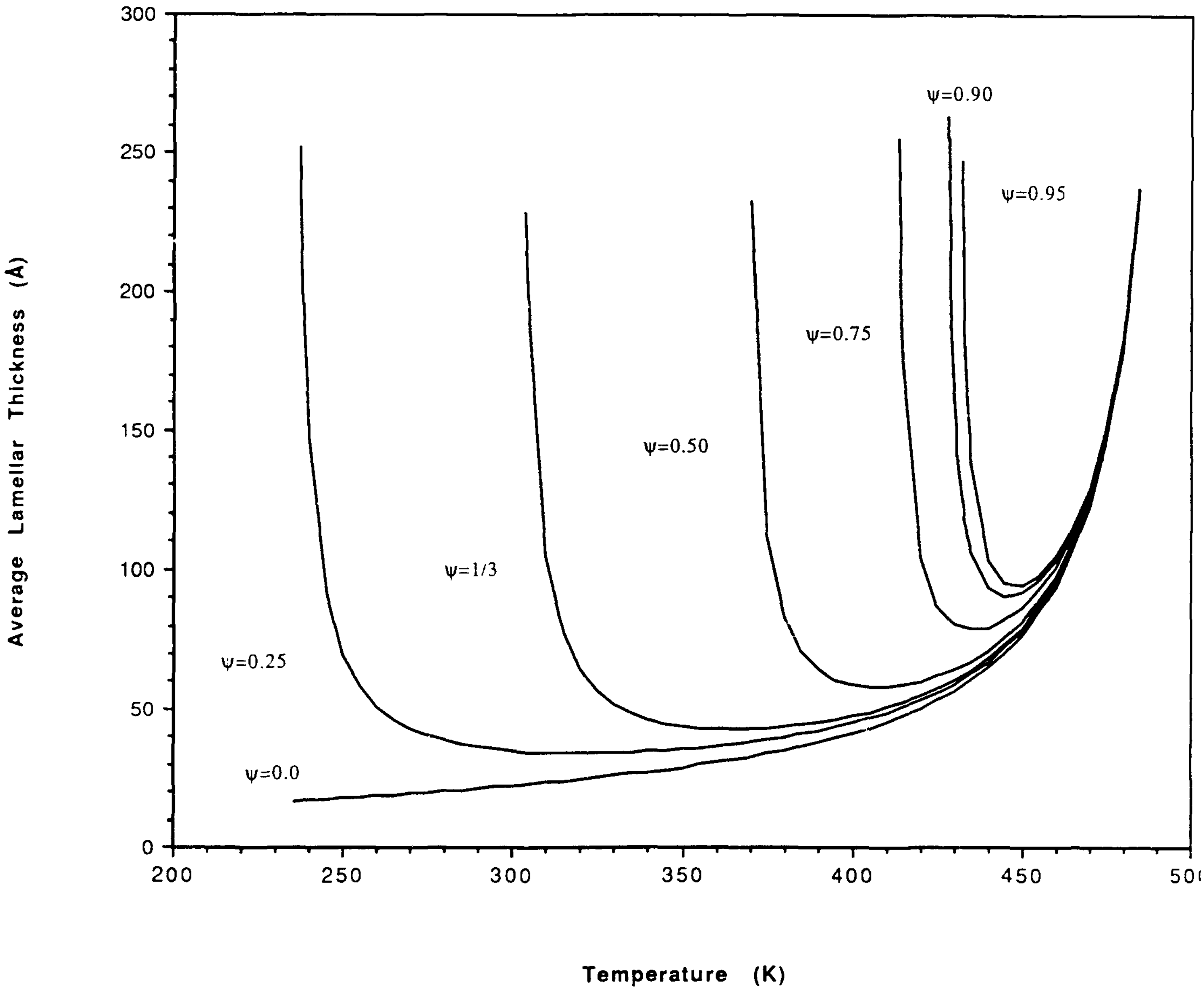

Average Lamellar Thickness (Å)
Temperature (K)
ψ=0.90
ψ=0.95
ψ=0.75
ψ=0.50
ψ=1/3
ψ=0.25
ψ=0.0
300
250
200
150
100
50
0
200
250
300
350
400
450
50

Figure 2.

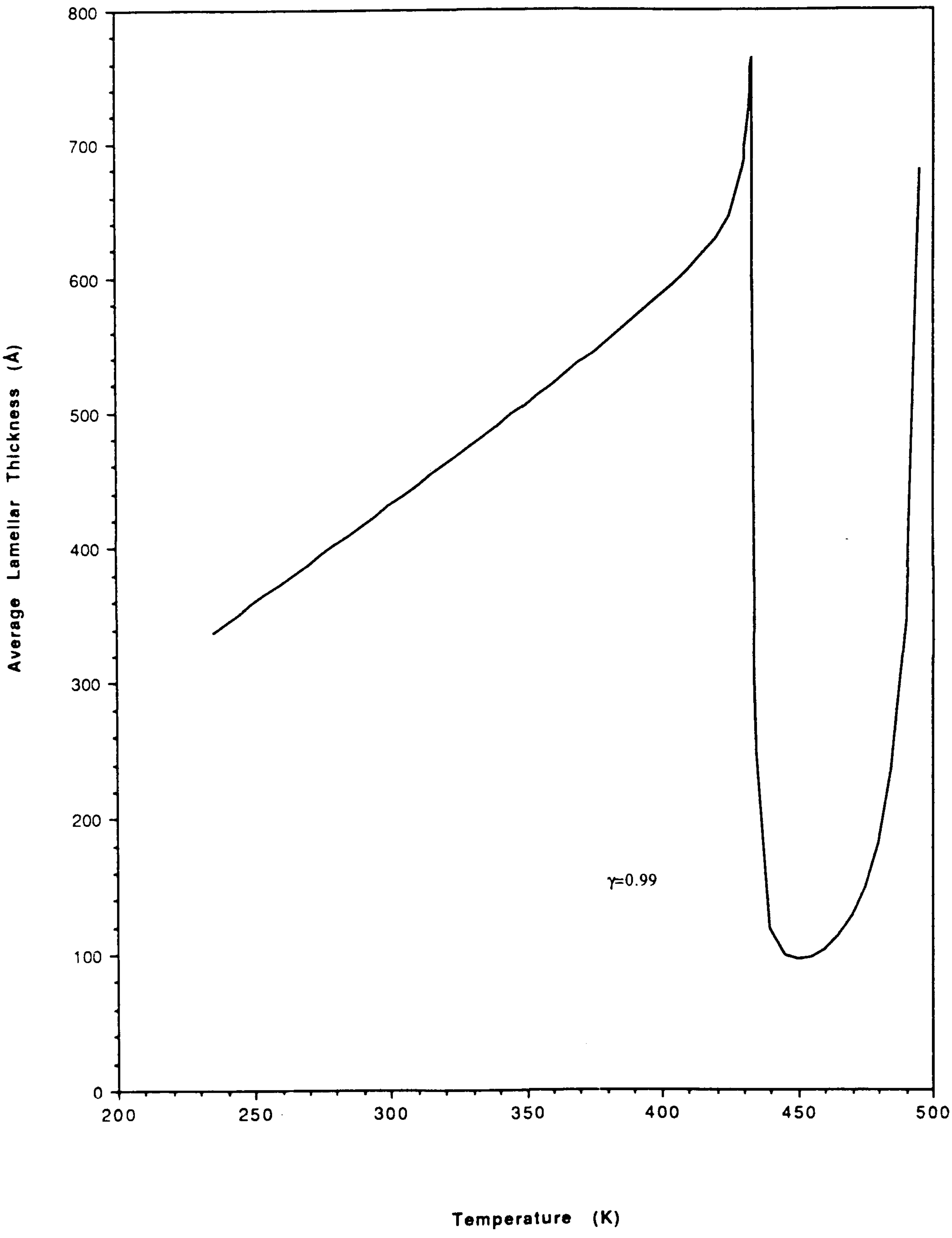

800
700
600
500
400
300
200
100
0
Average Lamellar Thickness (Å)
γ=0.99
200
250
300
350
400
450
500
Temperature (K)

Figure 3.

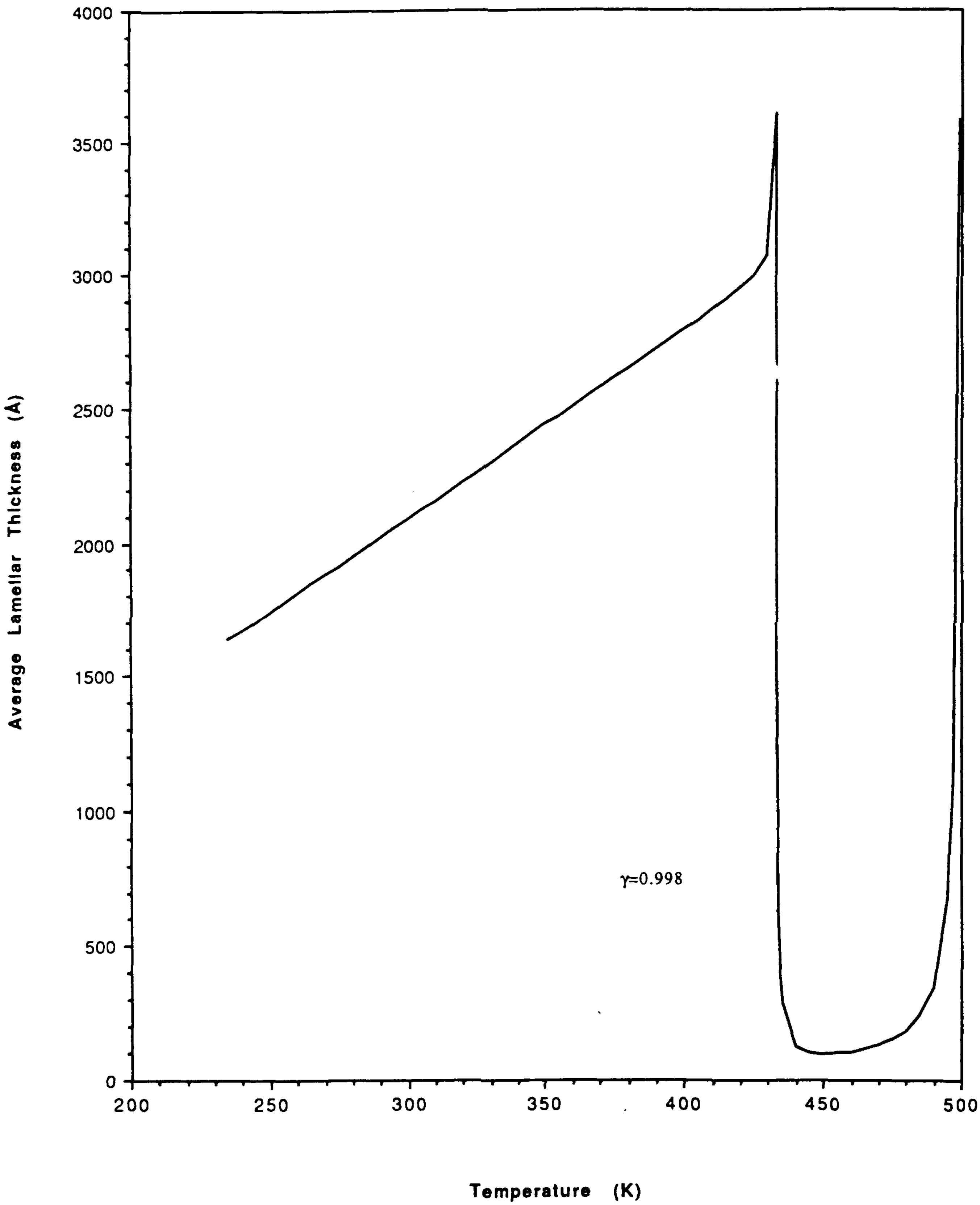
4000
3500
3000
2500
2000
1500
1000
500
0
Average Lamellar Thickness (Å)
γ=0.998
200
250
300
350
400
450
500
Temperature (K)

Figure 4.

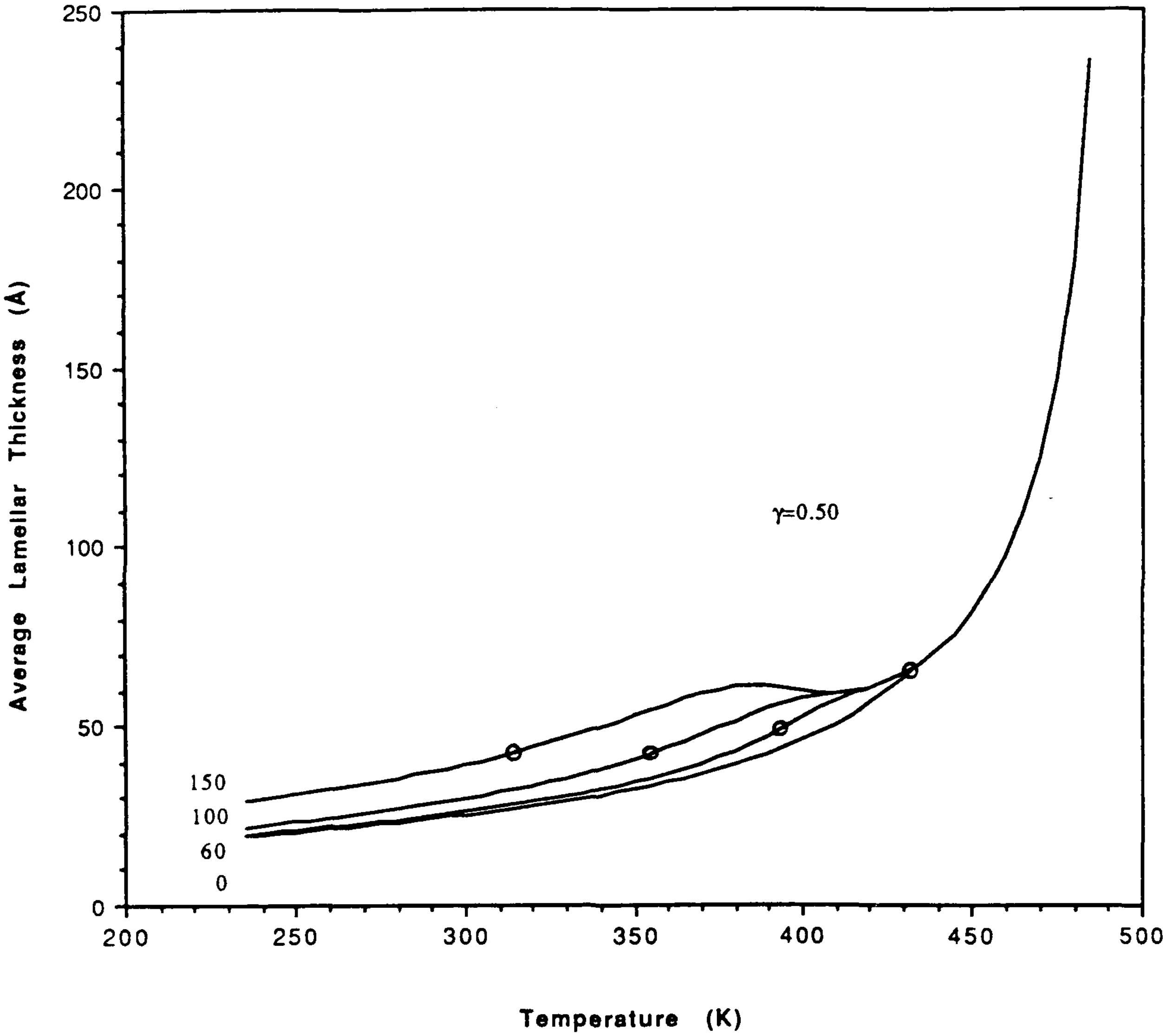

250
200
150
100
50
0
Average Lamellar Thickness (Å)
200
250
300
350
400
450
500
Temperature (K)
γ=0.50
150
100
60
0

Figure 5.

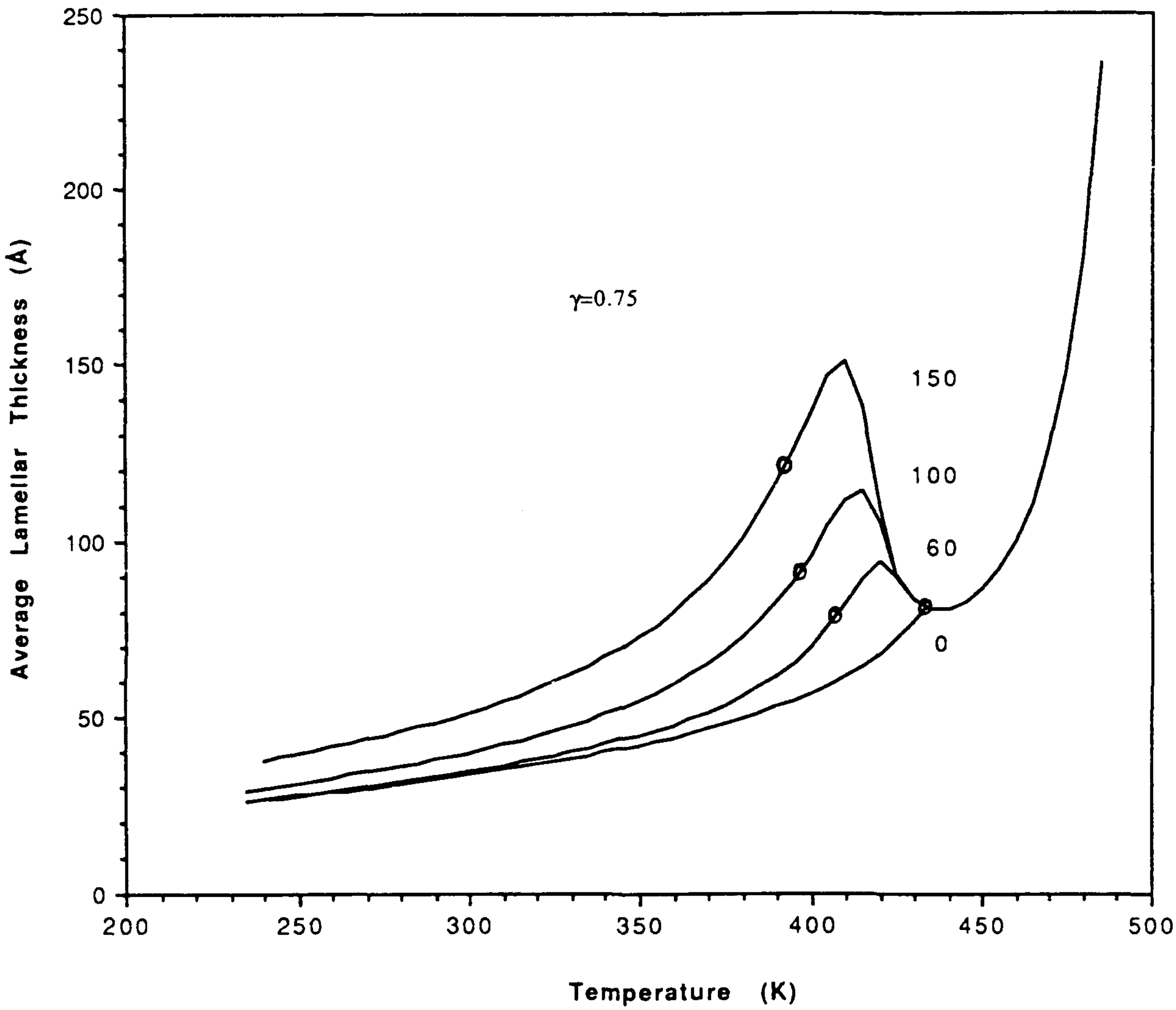

Average Lamellar Thickness (Å)
Temperature (K)
γ=0.75
150
100
60
0
250
200
150
100
50
0
200
250
300
350
400
450
500

Figure 6.

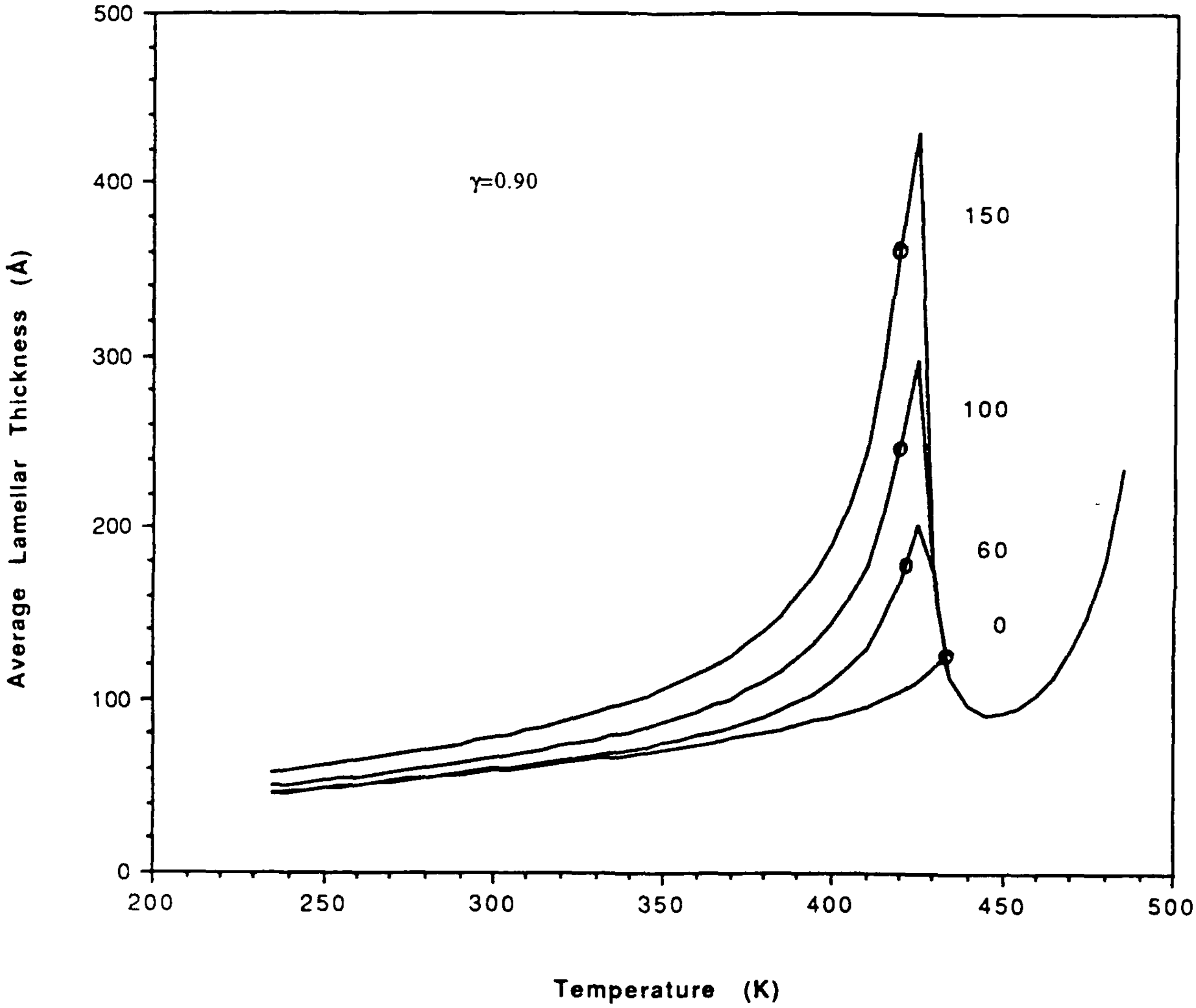

γ=0.90
150
100
60
0
Average Lamellar Thickness (Å)
Temperature (K)
0
100
200
300
400
500
200
250
300
350
400
450
500

Figure 7.

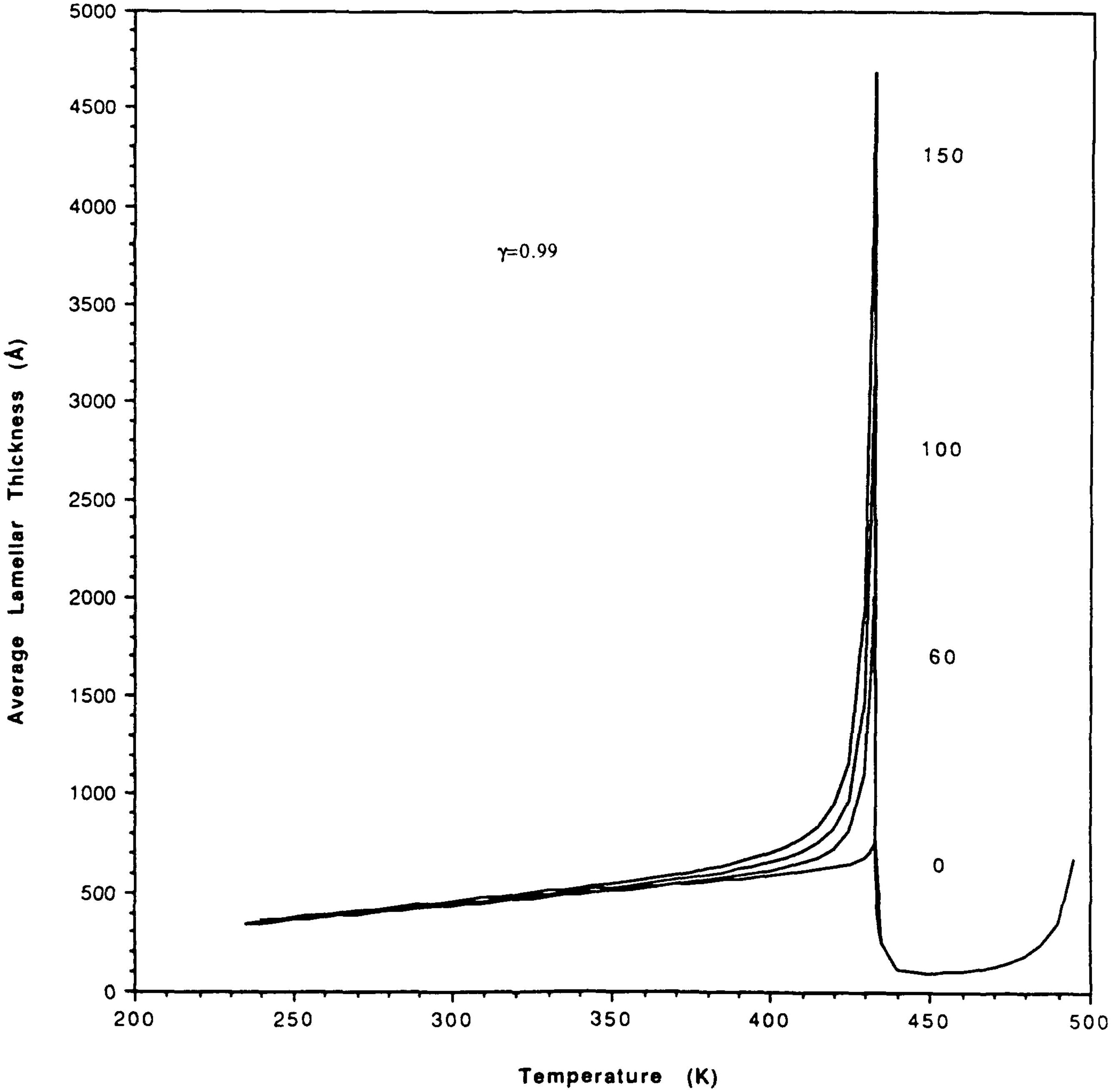
γ=0.99
150
100
60
0
5000
4500
4000
3500
3000
2500
2000
1500
1000
500
0
200
250
300
350
400
450
500
Average Lamellar Thickness (Å)
Temperature (K)

Figure 8.

Table I. Average Lamellar Thickness (Å) vs. Temperature (K)

TEMP. (K)	Psi=Gamma=0	Gamma=1/2	TEMP. (K)	Gamma=0.90
485.000	234.383	235.303	485.000	236.013
480.000	178.390	179.781	480.000	180.939
475.000	144.660	146.556	475.000	148.300
470.000	122.074	124.507	470.000	127.027
465.000	105.867	108.867	465.000	112.435
460.000	93.652	97.253	460.000	102.279
455.000	84.105	88.342	455.000	95.475
450.000	76.429	81.344	450.000	91.672
445.000	70.115	75.762	445.000	91.275
440.000	64.826	71.267	440.000	96.119
435.000	60.328	67.641	435.000	112.616
430.000	56.451	63.528	430.000	117.625
425.000	53.072	59.481	425.000	109.730
420.000	50.100	55.988	420.000	103.882
415.000	47.463	52.941	415.000	99.316
410.000	45.105	50.259	410.000	95.563
405.000	42.984	47.877	405.000	92.353
400.000	41.064	45.744	400.000	89.529
395.000	39.316	43.821	395.000	86.992
390.000	37.718	42.077	390.000	84.676
385.000	36.251	40.484	385.000	82.538
380.000	34.897	39.023	380.000	80.545
375.000	33.644	37.676	375.000	78.673
370.000	32.480	36.429	370.000	76.905
365.000	31.396	35.270	365.000	75.225
360.000	30.382	34.188	360.000	73.622
355.000	29.433	33.176	355.000	72.087
350.000	28.540	32.225	350.000	70.612
345.000	27.700	31.329	345.000	69.190
340.000	26.907	30.484	340.000	67.817
335.000	26.157	29.683	335.000	66.486
330.000	25.446	28.924	330.000	65.194
325.000	24.772	28.201	325.000	63.938
320.000	24.130	27.513	320.000	62.714
315.000	23.518	26.855	315.000	61.519
310.000	22.935	26.226	310.000	60.352
305.000	22.377	25.624	305.000	59.210
300.000	21.843	25.045	300.000	58.090
295.000	21.332	24.489	295.000	56.992
290.000	20.841	23.953	290.000	55.913
285.000	20.369	23.437	285.000	54.853
280.000	19.915	22.938	280.000	53.809
275.000	19.479	22.456	275.000	52.782
270.000	19.057	21.990	270.000	51.769
265.000	18.651	21.537	265.000	50.770
260.000	18.258	21.099	260.000	49.784
255.000	17.878	20.673	255.000	48.810
250.000	17.511	20.259	250.000	47.847
245.000	17.155	19.856	245.000	46.895
240.000	16.809	19.463	240.000	45.953
235.000	16.475	19.081	235.000	45.021

Table II. Average Lamellar Thickness (Å) vs. Temperature (K)

TEMP. (K)	LH Psi=1/2	LH Psi=0.90
485.000	235.785	237.166
480.000	180.224	182.177
475.000	146.926	149.552
470.000	124.780	128.225
465.000	109.027	113.507
460.000	97.290	103.129
455.000	88.251	95.962
450.000	81.124	91.560
445.000	75.412	90.139
440.000	70.789	93.098
435.000	67.037	105.777
430.000	64.009	160.924
425.000	61.610	∞
420.000	59.786	
415.000	58.519	
410.000	57.832	
405.000	57.800	
400.000	58.577	
395.000	60.458	
390.000	64.019	
385.000	70.494	
380.000	82.999	
375.000	112.171	
370.000	232.547	
365.000	∞	
360.000		
355.000		
350.000		
345.000		
340.000		
335.000		
330.000		
325.000		
320.000		
315.000		
310.000		
305.000		
300.000		
295.000		
290.000		
285.000		
280.000		
275.000		
270.000		
265.000		
260.000		
255.000		
250.000		
245.000		
240.000		
235.000		

Table III. Average Lameller Thickness (Å) vs. Temperature (K)

TEMP. (K)	Theta=1
495.000	675.848
490.000	
485.000	230.877
480.000	
475.000	142.184
470.000	
465.000	104.542
460.000	
455.000	84.037
450.000	
445.000	71.460
440.000	
435.000	63.333
430.000	
425.000	56.368
420.000	
415.000	50.779
410.000	
405.000	46.332
400.000	
395.000	42.690
390.000	
385.000	39.639
380.000	
375.000	37.036
370.000	
365.000	34.779
360.000	
355.000	32.796
350.000	
345.000	31.035
340.000	
335.000	29.454
330.000	
325.000	28.022
320.000	
315.000	26.716
310.000	
305.000	25.516
300.000	
295.000	24.405
290.000	
285.000	23.373
280.000	
275.000	22.407
270.000	
265.000	21.501
260.000	
255.000	20.646
250.000	
245.000	19.836
240.000	
235.000	19.067

Table IV. Average Lamellar Thickness (Å) vs. Temperature (K)

TEMP. (K)	0.5 // 60	0.5 // 100	0.5 // 150
485.000	235.303	235.303	235.303
480.000	179.781	179.781	179.781
475.000	146.556	146.556	146.556
470.000	124.507	124.507	124.507
465.000	108.867	108.867	108.867
460.000	97.253	97.253	97.253
455.000	88.342	88.342	88.342
450.000	81.344	81.344	81.344
445.000	75.762	75.762	75.762
440.000	71.267	71.267	71.267
435.000	67.641	67.641	67.641
430.000	64.735	64.735	64.735
425.000	62.454	62.454	62.454
420.000	60.723	60.743	60.743
415.000	59.214	59.577	59.584
410.000	57.306	58.874	59.005
405.000	54.856	58.337	58.984
400.000	52.149	57.582	59.533
395.000	49.469	56.411	60.296
390.000	46.971	54.852	60.919
385.000	44.708	53.035	61.120
380.000	42.683	51.095	60.800
375.000	40.874	49.136	60.003
370.000	39.252	47.220	58.842
365.000	37.791	45.385	57.434
360.000	36.466	43.648	55.882
355.000	35.253	42.015	54.261
350.000	34.136	40.486	52.625
345.000	33.100	39.056	51.009
340.000	32.131	37.719	49.436
335.000	31.219	36.468	47.918
330.000	30.358	35.295	46.462
325.000	29.541	34.194	45.072
320.000	28.766	33.159	43.746
315.000	28.028	32.183	42.485
310.000	27.324	31.262	41.286
305.000	26.652	30.390	40.145
300.000	26.009	29.564	39.059
295.000	25.392	28.778	38.025
290.000	24.799	28.031	37.040
285.000	24.229	27.318	36.101
280.000	23.681	26.637	35.204
275.000	23.152	25.985	34.346
270.000	22.641	25.360	33.526
265.000	22.147	24.760	32.740
260.000	21.669	24.184	31.986
255.000	21.206	23.628	31.263
250.000	20.756	23.093	30.567
245.000	20.320	22.576	29.898
240.000	19.896	22.076	29.253
235.000	19.484	21.593	28.631

Table V. Average Lamellar Thickness (Å) vs. Temperature (K)

TEMP. (K)	0.90 // 60	0.90 // 100	0.90 // 150
485.000	236.013	236.013	236.013
480.000	180.939	180.939	180.939
475.000	148.300	148.300	148.300
470.000	127.027	127.027	127.027
465.000	112.435	112.435	112.435
460.000	102.279	102.279	102.279
455.000	95.475	95.475	95.475
450.000	91.672	91.672	91.672
445.000	91.275	91.275	91.275
440.000	96.119	96.119	96.119
435.000	112.616	112.616	112.616
430.000	174.477	176.464	176.575
425.000	201.468	297.598	429.985
420.000	167.419	248.786	364.401
415.000	144.110	205.816	292.407
410.000	128.691	177.388	245.551
405.000	117.747	157.689	213.621
400.000	109.503	143.241	190.563
395.000	103.012	132.137	173.106
390.000	97.724	123.283	159.389
385.000	93.301	116.014	148.284
380.000	89.520	109.905	139.076
375.000	86.231	104.670	131.286
370.000	83.324	100.111	124.586
365.000	80.723	96.086	118.740
360.000	78.366	92.490	113.578
355.000	76.210	89.245	108.971
350.000	74.218	86.289	104.820
345.000	72.363	83.577	101.051
340.000	70.621	81.071	97.602
335.000	68.974	78.739	94.427
330.000	67.408	76.559	91.485
325.000	65.912	74.510	88.746
320.000	64.477	72.574	86.182
315.000	63.097	70.740	83.773
310.000	61.765	68.993	81.500
305.000	60.477	67.325	79.347
300.000	59.227	65.728	77.301
295.000	58.013	64.193	75.351
290.000	56.831	62.714	73.487
285.000	55.678	61.287	71.700
280.000	54.551	59.905	69.982
275.000	53.448	58.566	68.329
270.000	52.367	57.264	66.733
265.000	51.307	55.998	65.190
260.000	50.265	54.763	63.695
255.000	49.241	53.558	62.244
250.000	48.233	52.380	60.834
245.000	47.240	51.226	59.462
240.000	46.261	50.096	58.124
235.000	45.295	48.987	56.819